Orthopädische Klinik und Poliklinik, Universitätsmedizin Rostock

(Direktor: Prof. Dr. med. habil. Wolfram Mittelmeier)

Title:

Biomechanical Importance of Proximal Human Femur Morphology and Mechanics in Orthopaedic Purposes

Cumulative Dissertation
to
obtain the academic degree
"Doctor rerum humanarum" (Dr. rer. hum.)
at the Universität Rostock

submitted by
Ehsan Soodmand
born on 30.06.1985 in Ahvaz, Iran

Rostock, November 2019

Dean of Medical University of Rostock: Prof. Dr. med. univ. Emil C. Reisinger

First Reviewer:
Prof. Dr. med. habil. Dipl.-Ing. Rainer Bader, Department of Orthopaedics,
Universitätsmedizin Rostock, Germany

Second Reviewer:
Prof. Dr. med. Marc-André Weber, Institute of Diagnostic and Interventional Radiology,
Pediatric Radiology and Neuroradiology, Universitätsmedizin Rostock, Germany

Third Reviewer:
Prof. Dr. Peter Augat, Institute of Biomechanics, Berufsgenossenschaftliche Unfallklinik
Murnau, Germany and Paracelsus Medizinische Privatuniversität Salzburg, Austria

Submision date : November 2019
Defence date   : July 2020

Table of Content

List of Tables

Table of Equations

Table of Figures

1 Introduction

1.1 Importance of human femur in orthopaedics biomechanics

The human femur is the largest and strongest bone in human body, and is able to bear up to 30 times of human body weight (Arun and Jadhav, 2016). Since human femur is connected to both hip and knee joints, it plays a key role in the biomechanics of gait and posture linking lower limbs to upper limbs. Therefore, malfunctioning of femur results in a limitation of the human physical activities (Jensen, 1993). The connection of lower and upper limbs is possible through the proximal part of femur, which consists of head, neck, greater and lesser trochanters (Khaleel and Shaik, 2014). The head of femur medially articulates with acetabulum, and is covered by cartilage except in a depression, the fovea, on its medial side. The fovea serves for attachment of ligament of femoral head. The femoral neck connects the head to the shaft at an angle of nearly 120°. This enables the movement of hip joint and allows the lower limb to swing to the pelvis (Khaleel and Shaik, 2014). Since 60 % of all annual worldwide hip fractures occur in the neck area (Basso et al., 2012), the dimension of neck, its angle with shaft, and the correlation to other morphological parameters are essential for consideration in orthopaedics surgeries.

The annual worldwide occurrence of hip fractures reported to exceed 1.7 million (Woolf and Pfleger, 2003), and it is estimated to increase to 2.6 million in 2025 (Gullberg et al., 1997). These statistics present a major public health crisis, which is accompanied by a massive socioeconomic load and medical challenges. Biomechanical scientists have long been assessing the mechanical properties of human femurs and implants to address a vast range of orthopaedic conditions and traumatic injuries. To this end, orthopaedic surgeons have to choose the most effective implant to treat such fractures, which requires a good understanding of femoral geometrical properties as a first step.

1.2 Relevance of anatomical and morphological knowledge in orthopaedic biomechanics

The morphology of the femur is directly connected to biomechanical factors which have clinical impact. Orthopaedic surgeons performing total hip replacement (THR) must be aware of the biomechanical behaviour and the physiological functions of hip joint while using preoperative planning (Crooijmans et al., 2009, Sariali et al., 2009). For example, the length of the femoral neck is important as it determines the lever arm of muscles attached to the greater trochanter with respect to the centre of rotation of the hip joint, and it is connected to femoral offset (Lecerf et al., 2009). Disregarding the femoral offset was also shown to result in limited functional outcome and pain following THR (Clement et al., 2016). Abnormal morphology like joint deformity was observed to affect the development of early osteoarthritis, e.g. in case of high neck-shaft angle (NSA) (Labronici et al., 2015). The outcome of THR is also affected by the neck-shaft angle (NSA), therefore better investigation of NSA can effectively anticipate the incidence of femur fracture (Gnudi et al., 2012) in particular when osteoporotic (Pawaskar et al., 2012). Other morphological parameters like femoral head diameter (FHD) and anteversion angle (ATA) have an influence on range of motion (ROM) of the hip joint. Orthopaedic surgeons adjust the neck-shaft angle, vertical offset (OSV) and horizontal offset (OSH) by appropriate selection of type, size and model of total hip stem and head. In contrast, hip resurfacing arthroplasty (HRA), where only the cartilage surface is replaced by a metal cap, the surgeon requires to deal with the given morphology of the femur and has only a minor influence on changing relevant parameters. Femoral offset and the head-neck ratio affect the joint ROM and integrity of the artificial hip concerning femoroacetabular impingement (Bagwell et al., 2016). Assessment of anteversion angle (ATA) of the femoral neck is also crucial for positioning of hip replacement (Malik et al., 2007), and can reduce postoperative malrotation

after intramedullary nailing of femoral shaft fractures (Lindsey and Krieg, 2011). In addition, ATA has a remarkable influence on the incidence of osteoarthritis and hip dysplasia (Li et al., 2014). Therefore, analysis of abnormalities in femoral shape and orientation can contribute to predict orthopaedic diseases such as degenerative diseases, osteoarthritis (Li et al., 2014). According to all above-mentioned research findings, the accurate description of angles and bone dimensions is regarded crucial to design nails, plates and orthopaedic prosthetic or preoperative planning (Lindsey and Krieg, 2011, Ravichandran et al., 2011), and establishment of a comprehensive overview of femoral morphological parameters has become a focus in hip joint related treatments such as hip resurfacing arthroplasty over the last decade (Jack et al., 2013). Since the diversity observed in femur morphology is challenging, orthopaedic surgeons and engineers require a comprehensive overview for preoperative planning consideration as well as optimized prosthetics design enhancement. Several studies have been performed to investigate femoral geometrical parameters (Beck et al., 2005, Clement et al., 2016, Gregory and Aspden, 2008, Kluess et al., 2007, Li et al., 2014, Patton et al., 2006, Ravichandran et al., 2011). However, few groups suggest a complete set of parameters including their correlation and surgical relevance. Due to the limited access to these data , more comprehensive knowledge of femoral morphology is vital to deal with modern medical issues such as impingement after THR (Kluess et al., 2007) and HRA (Yoo et al., 2011), the aetiology of hip fracture (Patton et al., 2006), and proper design for orthopaedic implants (Baharuddin et al., 2014). Postoperatively, bone-implant mismatch is the main reason for several medical issues such as thigh pain, aseptic loosening or impingement (Kluess et al., 2007).

Therefore, the present work aims to analyse the femoral morphology with a reliable statistical approach for twelve essential morphological parameters of the proximal human femur. A detailed discussion on the clinical relevance of these parameters is then presented. This part of the work will provide an interpretation of importance of the morphological relevance of the proximal femur more accessible to clinicians with no particular background in biomechanics. The data presented can be used in different medical/biomedical research areas.

1.3   Accuracy assessment of image-based 3D reconstruction for biomechanical applications

Orthopaedic biomechanical research is based on four methodologies, *in-vitro* experiments, *in-vivo* animal studies, *in-situ* clinical observations, and *in-silico* computational analysis. To examine the biomechanical behaviour of human joints and tissues in clinical applications, subject-specific image based finite element analysis (FEA) has most commonly been used for *in silico* computational analysis (Pauchard et al., 2016, Taylor and Prendergast, 2015). Extraction of bone geometry from medical images, generation of an optimum finite element mesh, assigning proper material properties, and definition of actual boundary conditions are the main inputs for FEA (Pahr and Zysset, 2009), and consequently their accuracy affects the precision of the FEA result (Cattaneo et al., 2001). The first milestone of construction workflow of image-based biomechanical analysis is the accurate segmentation (extraction of preferred bone geometry from medical image data) from source data (Kang et al., 2014, Pinheiro and Alves, 2015, Van den Broeck et al., 2014). It is fundamental to obtain segmented bone data as authentic as possible to the patient's morphology. Since there are many commercial segmentation software packages and algorithms, The STL models segmented with commercially available software packages may have discrepancies compared to the real bone, and the accuracy of the segmented bone could then vary based on the segmentation method and operator's skills. Hence, the accuracy assessment of 3D reconstructed bone based on medical images has recently been extensively investigated (Choi et al., 2002, Eckstein et al., 2005, Fitzwater et al., 2011, Lalone et al., 2015, Oka et al., 2009, Pan et al., 2014, Pinsky et al., 2006, Shu et al., 2014, Wang et al., 2009, Wang et al., 2006, White et al., 2008, Gelaude

et al., 2008, Kang et al., 2014). Yet, it is concerned that such segmented models do not represent the accuracy of the original bone in a finite element model (FEM). Therefore, the effect of using different segmentation methodologies will be investigated, which were conducted by experts from seven biomechanics laboratories with different experiences and skills through a round robin test.

1.4   The necessity of a round-robin numerical analysis (FEA) in orthopaedic biomechanics

The numerical investigations of bone mechanics using FEA have widely been published for decades since FEA can be used to address many research questions in orthopaedic biomechanics such as the stress distribution after total joint replacement (Waanders et al., 2011), bone remodelling according to Wolff's law (Behrens et al., 2009, Weinans et al., 1994), the fracture risk of bone under specific loads and pathologies (Hambli et al., 2012, Zysset et al., 2015), and the treatment of bone fractures with ostesyntheses (Fan et al., 2018). FEA processes should be always verified to ensure that the results are accurate, reliable, and reproducible. The steps of analysing a case in FEA such as 3D reconstruction, meshing, assignments of material properties, defining boundary conditions, and applying the loads are very influential since any of these steps could simply change the results of FEA. On the other hand, the outcome of the FEA should be always validated with an experimental replica.

For quality assurance, there are certain processes in FEA that should be performed as standard procedures: First, it is necessary to justify the finite element mesh density and perform a convergence analysis. For some uncertain input parameters, a sensitivity analysis should be performed to assess whether the small changes in the input parameters show an unusually high impact on the results. The results should be then checked towards plausibility, e.g. by comparison with literature data. Finally, an experimental replica of the simulation or parts of the simulation is required to verify the numerically determined results. These minimum requirements for quality assurance of FE simulations have relatively prevailed in biomechanical bone research. However, to the best of author's knowledge, there is no round-robin FEA of long human bones with more than two participating biomechanics laboratories published yet, where the results of the experimental test were not known in advance. Helgason et al. (2008) have already emphasized on the development of a benchmark study in 2008. Nevertheless, only one comparative study on the lumbar spine has been published (Dreischarf et al., 2014), but all FE models compared in this study presented different specimens. Thus, in the last episode of this research a benchmark study will be performed to find out whether comparable results using similar bone sample are achievable from the different participating laboratories following a well-defined procedure. For this purpose, first a compression test was carried out using a human femur to measure strains and displacements. The experts of seven different participating laboratories in this study from Germany and Austria were then requested to perform a FEA based on a well-defined protocol without knowing the experimental results. Subsequently, the experimentally obtained data were compared with the numerical results predicted by each individual participating laboratories to verify how accurate the numerical results are in comparison with the experimental results considering different techniques.

2   Aims and Objectives

Since the geometry of anatomical landmarks plays a very important role in the biomechanical analysis for orthopaedic purposes, a good and precise understanding of these landmarks is crucial for orthopaedic surgeons and biomechanical engineers. Therefore, an appropriate database is required to present morphological parameters and the correlations among them considering surgical issues. Moreover, numerical analysis as a major tool of preclinical biomechanical analysis should be performed considering accurate anatomical landmarks. Therefore, the reconstructed 3D bone models should be accurately reconstructed, and the assumptions, boundary condition, meshing algorithms, analysis algorithms, and simulation of applied loads should be also precisely defined. Thus, a quantified accuracy assessment of 3D reconstructed models based on the real bone geometry considering all morphological landmarks is required to assure the orthopaedic surgeons that biomechanical modelling is reliable. Furthermore, numerical analysis of orthopaedic procedures needed to be validated with comparison to the experimental analysis of real human bone. Regarding all the above-mentioned concerns, in the accuracy assessment procedure, apart from comparing the numerical outcome with the experimental data of real bone, the influence of human expertise, capability of software packages, surface meshing algorithms, applied material laws, and material mapping on the computational model will be investigated. Hence, the following aims were sought to be achieved in the present work:

Aim 1: to provide a database of surgically important morphological parameters of proximal human femur for orthopaedic and biomedical research purposes

Aim 2: to understand how the 3D reconstructed images deviate from the optical 3D scan of real human femur;

Aim 3: to investigate the accuracy and reliability of the developed image-based finite element model in comparison with the experimental results.

In the first study (publication 1), a database of surgically relevant morphological parameters and their correlations is provided, which are relevant for medical questions such as impingement after total hip replacement, implant design, and the aetiology of hip fracture. Twelve well-known morphological parameters of the human femur in 169 healthy human subjects through evaluation of 3D-reconstructed CT scans were investigated. The Pearson's coefficients of correlations were calculated using a statistical t-test method for each pair of parameters.

The second study (publication 2) contrasts the accuracy of different reconstructed models with distinctive segmentation methods performed by various experts. Seven research groups reconstructed nine 3D models of one human femur based on an acquired CT image using their own computational methods. As a reference model for accuracy assessment, a 3D surface scan of the human femur was created using an optical measuring system. Prior to comparison, the femur was divided into four areas; "neck and greater trochanter", "proximal metaphysis", "diaphysis", and "distal metaphysis". The deviation analysis was carried out using specific software.

In the third study (publication 3), a fresh-frozen human femur was prepared for a compression test in a universal testing machine measuring the strains at 10 bone locations as well as the deformation of the bone in terms of the displacement of the loading point. The laboratories blinded to the experimental results were asked to perform a finite element analysis simulating the experimental setup and deliver their results (strains and deformation) to our institution.

3 Material and Methods

3.1 Specimen and CT image acquisition (Study 1, 2, and 3)

In the current work, 170 adult healthy human femurs were used for the biomechanical investigations. The first study was performed on 169 human femurs where computed topography (CT) images of the bones obtained in supine position with slice thickness of 0.625–1.5mm and a pixel size of 0.652–1.087mm. CT images of 129 femurs were acquired at the University of Bern, Switzerland, and the other 40 CT scans were obtained at University of L beck, Germany (55% females and 45% males with average age of 71.9 years).

The second and third studies were performed on one right femur of a 58 year-old male cadaver. The bone was provided and the CT image acquired by Trauma Center Murnau, Germany. The CT image was saved as DICOM with resolution of 0.29 × 0.29mm and slice thickness of 0.6mm for deviation analysis.

3.2 Definition of the Morphological Parameters of Proximal Human Femur (Study 1)

The frontal, sagittal, and transversal planes (Figure 1) were defined on the 3D reconstructed models of femoral bones. Twelve descriptive parameters for the proximal femur were then selected as shown in Figure 2 and Figure 3.

The parameters are as follows:

1. Femoral head diameter (**FHD**). The diameter of best-fit sphere of the femoral head irrespective of its vertical or transverse orientation.

2. Total femur length (**TFL**). Distance between the most distal point in the transversal plane and a parallel plane containing the most proximal point of the femur.

3. Neck-Shaft angle (**NSA**): Angle made by axis of femoral shaft and the line which passes through the centre of femoral head along axis of femoral neck.

4. Anteversion angle (**ATA**): Angle between a transverse line passing through the femoral head and neck centre and an imaginary transverse line running medially to laterally through the knee joint.

5. Absolute offset (**OSA**): Distance between femoral head centre (FHC) and femoral shaft axis (FSA). Femoral shaft axis was constructed by selecting diaphysis part between 50 % and 80 % of the length of the femur (Figure 1).

6. Vertical offset (**OSV**): Vertical distance between FHC and the plane parallel to transversal plane containing the centre of the lesser trochanter.
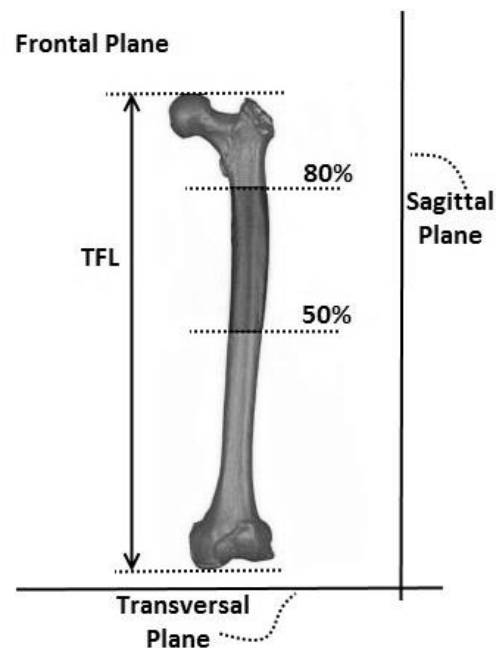
Figure 1 - Defined frontal, sagittal, and transversal planes. TFL indicates the total femoral length. 50% and 80% indicate half of the femoral length and 80% of femoral length from distal point respectively.

7. Horizontal offset (**OSH**): Projected distance between FHC and FSA to the frontal plane.

8. Greater trochanter height (**GTH**): Vertical distance between FHC and the plane parallel to the transversal plane containing the most proximal point of the greater trochanter.

9. Distance between FHC and femoral neck axis (FNA) projected to the sagittal plane (**NCDS**).

10. Distance between FHC and FNA projected to the frontal plane (**NCDF**).

11. Vertical distance between the FHC and a plane parallel to transversal plane containing the projection of the FHC to the FNA (**NCVD)**; positive for cranial positions of the FHC and negative for caudal positions.

12. Distance between the FHC and a plane parallel to the frontal plane containing the projection of the FHC to the FNA **(NCHD)**; positive for anterior position of the FHC and negative for posterior position.

a) Superior View   b) Lateral View
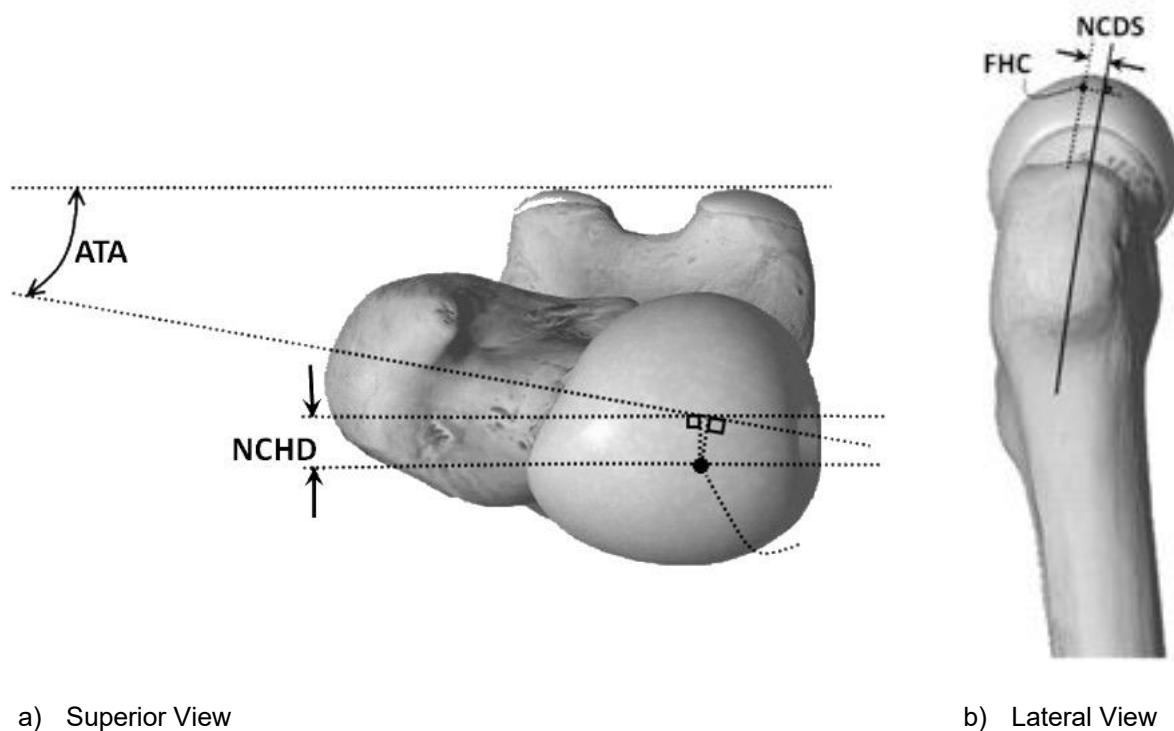
Figure 2 - a) Superior and b) lateral view of human femur and illustration of part of the defined morphological parameters as follows: ATA indicates anteversion angle; NCHD indicates the distance between the FHC and a plane parallel to the frontal plane containing the projection of the FHC to the FNA; FHC indicates femoral head center; NCDS shows the distance between FHC and femoral neck axis (FNA) projected to the sagittal plane. (The femur shape itself was reproduced using the freely available software called Essential Skeleton 4 (3D4Medical.com, 2014), however the defined parameters were specified and drawn by the authors).
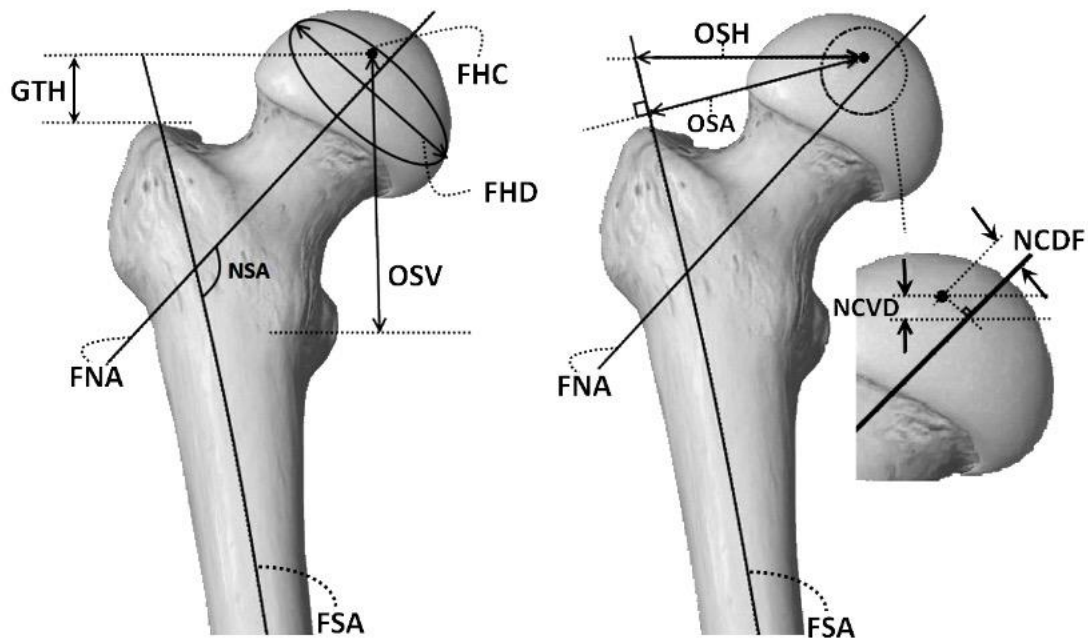
Figure 3 – Anterior view of human femur demonstrating morphological parameters defined as follows; GTH: Greater trochanter height, FHC: Femoral head canter, FHD: Femoral head diameter, NSA: Neck-Shaft angle FNA: Femoral neck axis, OSV: Vertical offset as the vertical distance between FHC and the plane parallel to transversal plane containing the centre of the lesser trochanter, FSA: Femoral shaft axis, OSH: Horizontal offset as the projected distance between FHC and FSA to the frontal plane, OSA: Absolute offset as the distance between femoral head centre (FHC) and femoral shaft axis, NCDF: Distance between the FHC and a plane parallel to the frontal plane containing the projection of the FHC to the FNA , NCVD: Vertical distance between the FHC and a plane parallel to transversal plane containing the projection of the FHC to the FNA (The femur shape itself was reproduce using the freely available software called Essential Skeleton 4 (3D4Medical.com, 2014) but the defined parameters were specified and drawn by the authors.

3.3   3D surface reconstruction of computed topography images (study 1 and 2)

In the first study, 129 femurs were segmented and 3D reconstructed at university of Bern using a combination of fast random forest regression-based landmark detection and atlas-based segmentation with an articulated statistical shape model instantiation (Chu et al., 2015). The statistical shape model of the femur was constructed using an in-house pipeline, which combined surface-based affine registration with intensity-based non-rigid registration to establish vertex-to-vertex correspondences between a randomly-selected reference model and all remaining femoral models. The constructed statistical shape model used in this study has also been successfully applied in a 2D−3D reconstruction application (Zheng et al., 2018), which demonstrated the validity of the constructed model. At Biomechanics and Implant Technology Research Laboratory (FORBIOMIT), commercial software, AMIRA® v.5.4.1 (FEI Visualization Sciences Group, Hillsboro, Oregon, USA), was used for reconstruction of a 3D model of human femurs from the CT images. The bony structures were labelled in all slices of the CT images based on the values of the Hounsfield unit (HU) for bones. Removal of the holes and sharp edges that were formed due to semi-automated segmentation was undertaken in AMIRA® v.5.4.1 using an established protocol (Kluess et al., 2009, Soodmand et al., 2018) to reconstruct the surfaces accurately.

In the second study, seven laboratories were asked to participate in the accuracy assessment study. DICOM files obtained from the CT scan of the aforementioned human femur were used to segment the surface by four different segmentation software packages: AMIRA® (FEI Visualization Sciences Group, Hillsboro, Oregon, USA), Mimics® (Materialise N.V., Leuven,

Belgium), YaDiv (Welfenlab, Leibniz Universit t Hannover, Hannover, Germany) (Friese et al., 2011), and Fiji Life-Line (Schindelin et al., 2012). The bone regions were labelled in all slices of the CT images based on the certain values of Hounsfield units (HU) for bones. The process of labelling of bony structures is a visual and subjective procedure in which a primary HU value for bones was selected from the literature which is approximately 200–250 up to 3000 (Ahmady et al., 2014, Kluess, 2010, Soodmand et al., 2015, Treece et al., 1999). The automated segmentation of the bone started by thresholds of HU and was followed by manually editing the slices to obtain more accurate surfaces (Ahmady et al., 2014, Kluess, 2010, Soodmand et al., 2015, Treece et al., 1999). A triangulated surface of the femurs was created with the segmentation software using a semi-automatic method. Removal of the holes and sharp edges which were formed due to semi-automated segmentation was implemented in the above mentioned software (Chu et al., 2015, Kluess, 2010, Kluess et al., 2008, Kluess et al., 2009). Software information, methods and duration of the segmentation process for each model are listed in Table 1.

Table 1 – Segmentation information such as segmentation software, time taken for segmentation, and segmentation method for each participant

Laboratory	Software	Time [min]	Segmentation Method
Laboratory 1	Mimics 18	480	Semi-automatic + Manuel Editing (3-Matic v.10)
Laboratory 2A	AMIRA® v.5.3.3	480	Semi-automatic + Manuel Editing (MeshLab 1.3.4)
Laboratory 2B	YaDiv 1.0 beta 5	480	Semi-automatic + Manuel Editing (MeshLab 1.3.4)
Laboratory 3	AMIRA® v.5.4.1	600	Semi-automatic + Manuel Editing
Laboratory 4	AMIRA® v.6	330	Semi-automatic + Manuel Editing (Geomagic Studio v.2012)
Laboratory 5	AMIRA® v.5.6	480	Semi-automatic + Manuel Editing (Geomagic Studio v.2012)
Laboratory 6	Fiji – Medtool v.4.0	85	Full-automatic + Manual Editing
Laboratory 7A	AMIRA® v.5.4.1	270	Semi-automatic + Manuel Editing (Geomagic Studio v.2013)
Laboratory 7B	Mimics v.17	340	Semi-automatic + Manuel Editing (3-Matic v.9)

3.4   *Optical 3D digitization of Human Femur (Study 2)*

To fulfil the aim of accuracy assessment of surface reconstruction in the second study, the outer geometry of the femur as a reference geometry of the bone was scanned using an optical measuring system at the Fraunhofer Application Centre of Large Structures in Production Engineering (AGP) in Rostock (Figure 4). The ATOS series of industrial optical 3D scanners (GOM - Gesellschaft für Optische Messtechnik mbH, Braunschweig, Germany) provide accurate scans with detailed resolution at high speeds. ATOS provides a full surface and primitives precisely in a dense point cloud or polygon mesh. Table 2 presents the specifications of the ATOS scanner for scanning the femur.

Table 2 – Optical 3D scanner system specifications. (Structured Light Projection System GOM ATOS III)

Measuring field (xyz) 500	500 x 500 (mm²)
Distance between points	0.24 (mm)
Accuracy (probing / spacing / flatness)	MV500: 0.009 / 0.030 / 0.017 (mm)
Resolution	2048 x 2048 (4 Megapixels)
Scan time	2.0 (s)
Dimensions	690 (W) × 220 (H) × 160 (D) (mm)

Figure 4 – Optical 3D scanning setup. The bone is located on the bench, scanning is performed by the optical scanner on the movable stand and controlled by the computer.

3.5 Deviation analysis of image-based reconstructed 3D models using an optical 3D digitized model (study 2)

In the second study, the accuracy of 3D reconstructed surfaces was assessed in comparison with the optical 3D scan of the human femur. Stereolithography (STL) files were collected from all project partners and imported into GEOMAGIC studio v.2013 (Raindrop Geomagic, NC, USA) for deviation analysis. Thereby, the researcher conducting the analysis was blinded towards the participant's identity to avoid bias. Prior to comparison, the femur was divided into 4 areas: "neck and greater trochanter" area, "diaphysis", "proximal metaphysis" and "distal metaphysis". Five different planes were defined in global coordinates to divide all models into above-mentioned areas.
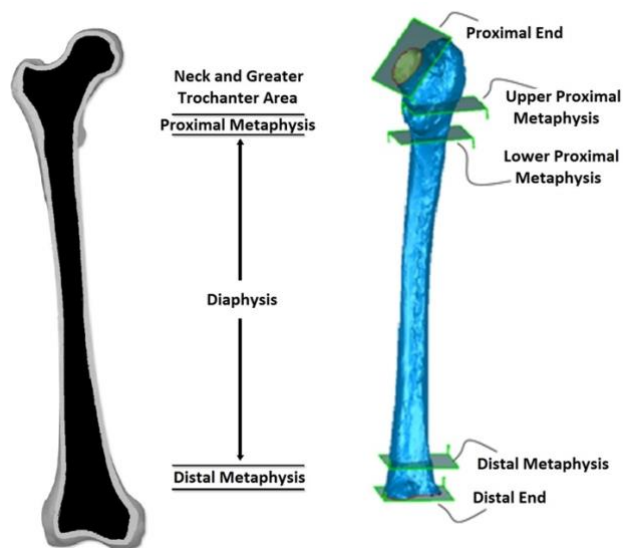
Figure 5 - Five predefined planes for splitting femur into 4 pieces to perform the deviation analysis.

Proximal end, upper proximal metaphysis, lower proximal metaphysis, distal metaphysis and distal end were the predefined planes for splitting the models into four aforementioned parts (BruceBlaus.com, 2014). Figure 5 illustrates the predefined cutting planes of the femur. The Neck area includes "neck and greater trochanter", and the "proximal metaphysis" contains the area of lesser trochanter. The "diaphysis" was defined as a long bone known as the femur shaft and the last part excludes the epiphysis called "distal metaphysis".

3.6 Biomechanical testing of the femur (study 3)

In study 3, the biomechanical testing was performed in Biomechanics and Implant Technology Research Laboratory (FORBIOMIT), Department of Orthopaedics, Rostock University Medical Center. The distal end of the human femur was embedded in casting resin in a metal embedding pot in order to fix the femur in an upright position (Figure 6a). A casting of the femur head was prepared with 10mm depth for load transferring to ensure the widest possible load transmission (Figure 6b). The casting mold was located between the femoral head and the metal plate applying displacement (Figure 6c). To determine the proper location for installing strain gauges, a preliminary finite element analysis (FEA) was performed to define the areas with the highest possible strain homogeneity.

10 linear strain gauges with one measurement grid (HBM, Darmstadt, Germany, a 1⁄4 9 106/K) were placed at 10 predefined locations (Figure 6d). Before placing the strain gauges on the sites, soft tissues were stripped off pre-treated with acetone, and primed with HBM X60 (HBM, Darmstadt, Germany). After preparing the application site, the strain gauges were glued using Loctite 4011 instant adhesive (Henkel Corp., Rocky Hill, CT, USA). There were eight locations in the femur diaphysis and two locations on the femoral neck, whereby one strain gauge was applied in the compression and one in the tension area (Figure 6c & d).
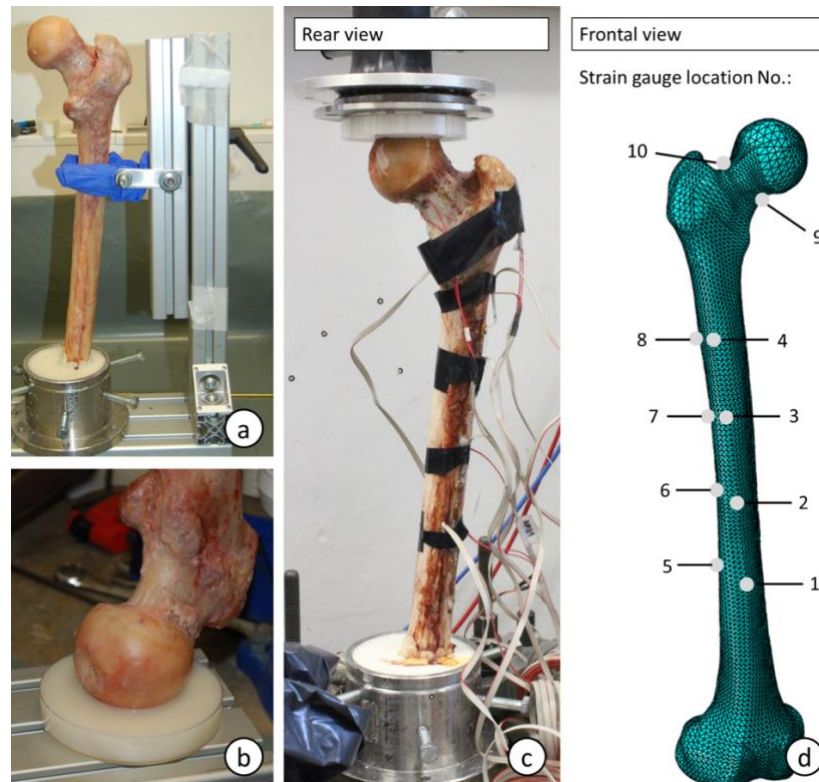
Figure 6 –Setup for biomechanical testing a) The femur was fixed using a tripod and embedded using casting resin in the embedding metal pot. The image indicating the orientation of the femur fixing in the embedding pot. b) The casting mold prepared for the femur head to optimize load transmission. c) The femur equipped with 10 strain gauges in the load frame of the testing machine. d) The locations of 10 strain gauges on the femur surface. The image is the outcome of preliminary FEA to estimate the best location of the strain gauge.

To measure the horizontal and vertical displacements of femoral head, a 20MP digital camera with 100 mm macro objective was fixed on a tripod in front of the testing machine while the loads applied to the femur. For calibration, an image was taken from a steel ruler in the same focal distance as the femoral head. At each loading level one image was captured by the camera. Vertical and horizontal displacements of femoral were evaluated using image correlation. The vertical displacement of femoral head direction was validated with the known traverse displacement of the testing machine.

A servohydraulic testing machine was used (Instron 8874 with software WaveMatrix, Instron GmbH, Darmstadt, Germany) to apply the loads to the femur. The embedding pot with femur was fixed with screws to the base of the testing machine. The femur was preloaded applying 50N. Then, compression loads on the femur from 200N to 2000N in 10 incremental steps were applied. To reach the desired value of the loading, each load stage was applied for 5 seconds to prevent viscoelastic phenomena. A digital camera was used to record the experiment.

The experiment was performed five times, and the experimental strains were measured during each repletion.

A high-resolution optical scan of the specimen was performed after the experiment as described in section 0 of this dissertation. The optical scans were captured to identify the position of the strain gauges. The positions of strain gauges were extracted from the reconstructed STL surface network, and prepared for the round-robin test protocol.

3.7 Finite element modelling of the human femur (study 3)

3D reconstructed model of the femur based on the CT image was meshed with quadratic, 10-node, tetrahedral finite elements (C3D10) using commercial software Abaqus/CAE® (v6.13-1, Dassault Syst mes Simulia Corp., Providence, Rhode Island, USA). An in-house mapping algorithm was used to assign Young's modulus to each node of the finite element model (FEM) based on the Hounsfield unit (HU) values of the CT image of the femur. To correlate the HU values of the CT image, a calibration phantom with a known bone mineral density (ρ_{ash}ash density) served as a reference for the linear regression:

$$\rho_{ash} = \frac{HU}{895.93}$$

Equation 1- Calculation of ash density with linear regression to the Hounsfield Unit values

The Young's modulus of bone was then assigned for each nodes according to its respective ash density based on the following equation presented by Cong et al. (2011).

$$E = 20000^{(-5.19)}(e^{(-2.30\rho_{ash})})$$

Equation 2- Young's modulus of bone based on the ash density

where E is the Young's modulus in GPa and ρ_{ash} is the ash density in $\frac{g}{cm^3}$ for each nodes of the FEM. Poisson's ratio was assumed to be v = 0.3 for the entire femur (Little et al., 2007). The values of less than 1MPa were assumed as 1MPa to avoid negative or zero elasticities in the FEM (Eberle et al., 2013).

As explained in section 0 of this dissertation, the position of strain gauges and boundary conditions (the location of encastered femur in the embedding pot) were identified using an optical 3D scanner. All the nodes of femoral bone below the encastered location were entirely constrained to zero degree of freedom (Figure 7). The compression load was applied to a reference point above the femoral head replicating the experimental compression loading (Figure 7). The force distributed the resulting displacement to the nodes of FEM on the upper part of the femoral head.

3.7.1 Guidelines given from the coordinator to the partners

In study 3, a round-robin finite element analysis (FEA) of the human femur was performed and seven different biomechanics laboratories were participated, where the results of the experimental tests were compared to their FEA results. A protocol was prepared by our institute to provide all necessary instructions to the other laboratories participating the round-robin test. All participants used their own anatomical geometry obtained from the CT data (Soodmand et al., 2018). All laboratories were asked to reproduce the situation of the experimental setup in their FEAs (Figure 7). The laboratories were advised to measure the average of the strains in the measuring area of strain gauges (2mm width and 3mm length). The direction of the strain corresponded to the axis normal to the embedment level except for the two strain gauges applied at the femoral neck. The detailed information of FEA obtained from all participating laboratories were listed in Table 3 including the software they used by them for the FEA, the specifications of their computers, the element types, number of element available in their FEM, material properties, and the boundary conditions.
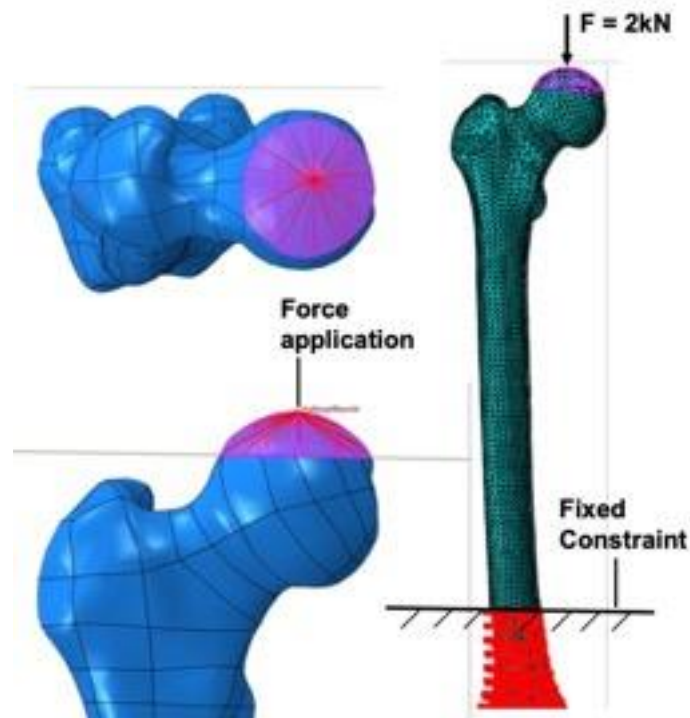
Figure 7 – Numerical simulation of the experimental condition in the finite element model indicating the femur, embedded part, the magnitude and direction of applied force, and the boundary conditions.

3.8 Statistical analysis

Minimum (Min), maximum (Max), mean, median, and standard deviation (SD) were calculated in Microsoft Excel 2013. Pearson's coefficients of correlation were calculated using a statistical t-test method in R v.3.2.2 (R Core Team, www.r-project.org) for each pair of morphological parameters. The significance level was set at $p < 0.05$.

Table 3 - Details of the partner lab's materials and methods for conducting the FEA of the human femur

Partners	Software	Specification of the computer	Element Numbers	Element Types	Material Properties	Simulation of distal embedding
Lab 1	ANSYS 17 (ANSYS Inc., Canonsburg, PA, USA)	Windows 7 Professional Intel® Core™ i7-960 CPU @3.20GHz 8GB RAM	1,061,670	10-node-tetrahedron, type SOLID187	Linear-elastic with $E = 17\ GPa$ $\mu = 0.3$	Cut at the embedding level with encastre boundary condition
Lab 2	Abaqus Version 6.13-1 (Dassault Systèmes Simulia Corp., Providence, RI, USA)	Windows 7 Professional Intel® Core™ i7-4790 CPU @3.60GHz 8GB RAM	72,153	10-node-tetrahedron, type C3D10	Trabecular bone: Mapping of CT-data on FE-mesh, nodewise definition of HU as temperature using temperature-dependent material model [8, 14]: $E = 20,000e^{-5.19e^{-2.30\rho_{ash}}}$ Cortical bone: Linear-elastic with $E = 17\ GPa, \mu = 0.3$ [15]	Cut at the embedding level with encastre boundary condition
Lab 3	Meshing: medtool v4.1 – "Bone Mesher" [16] Material mapping: medtool v4.1 – "CT Interpolator" [16] FEA Code: Abaqus V6R2017 (Dassault Systèmes Simulia Corp., Providence, RI, USA)	CentOS 7.4, Intel Core™ i7-4790 CPU @ 3.60GHz, 32GB RAM	73,817	Trabecular Bone: Tetrahedron, type C3D10 Cortical Bone: Wedge, type C3D15	Trabecular bone: Nonlinear, BMD-dependent, isotropic material mapping, extended UMAT from [17] Cortical bone: Linear-elastic with $E = 18,565\ MPa$ $\mu = 0.495$ [18]	Considering the distal femur below embedding level with encastring of embedded bone surface
Lab 4	ANSYS 18.1 (ANSYS, Inc., Canonsburg, PA, USA)	Windows 7 professional Intel® Xeon™ E5-2667 v3 CPU @3.20GHz 3.20GHz (2 Processors) 192GB RAM	3,273,912	10-node-tetrahedron, type SOLID187	Trabecular bone: Linear-elastic with $E = 1904\rho^{1.64}$MPa, v = 0.3 [15] Cortical bone: Linear-elastic with $E = 2065\rho^{3.09}$MPa, v = 0.36 [15]	Considering the distal femur below embedding level with encastring of embedded bone surface
Lab 5	ANSYS 18.1 (ANSYS Inc., Canonsburg, PA, USA)	Windows 7 Professional, Intel® Xeon® CPU E5-2687W 0 @ 3.10GHz, 128 GB RAM	1,421,638	10-node-tetrahedron, type SOLID187; SHELL281 (stress/strain evaluation only)	Both cortical and trabecular bone: Isotropic but inhomogeneous elasticity properties, mapping of HU units from CT-data on FE-mesh, nodewise definition of HU as temperature using temperature-dependent material model [10, 19, 20]: $E = 12486\ \rho_{qCT}^{1.16}$	Considering the distal femur below embedding level with encastring of embedded bone surface
Lab 6 I	ANSYS 18.1 (ANSYS Inc., Canonsburg, PA, USA)	Windows 7 professional, 2x Intel® Xeon™ E5-2650 CPU @2.00GHz, 32GB RAM	158,450 (only femur)	10-node-tetrahedron, type SOLID187	Total of 13 material cards with new material data every 2,000 MPa in transition region. $\rho_{qCT} = -0.0130 + 0.000977HU$ $\rho_{qCT} < 0.26\ g/cm^3 \rightarrow E = 0\ MPa$ $0.26 g/cm^3 < \rho_{qCT} < 0.66\ g/cm^3 \rightarrow E = 6,850\rho_{app}^{1.49}$ $\rho_{qCT} > 0.66\ g/cm^3 \rightarrow E = 22,700\ MPa$ $\rho_{app} = 1.82\rho_{qCT}$ $\mu = 0.3$ [10, 21-23]	Embedding medium was modeled as deformable solid, contact condition between embedding medium and bone
Lab 6 II	ANSYS 18.1 (ANSYS Inc., Canonsburg, PA, USA)	Windows 7 professional, 2x Intel® Xeon™ E5-2650 CPU @2.00GHz, 32GB RAM	147,030 (only femur)	10-node-tetrahedron, type SOLID187		
Lab 7	ANSYS 18.1 (ANSYS Inc., Canonsburg, PA, USA)	Windows Server 2016 Standard Intel® XEON® Gold 5122 CPU @3.60GHz 3.59 GHz (2 Prozessoren) 128 GB RAM	4,336,885	10-node-tetrahedron, type SOLID187	Mapping of CT-data on Femur-FE-mesh, nodewise definition of HU as elastic model [24]: $E[MPa] = 2,875 \cdot \left(\frac{2 \cdot HU}{HU_{max}}\right)^3$	Cut at the embedding level with encastre boundary condition

4 Results

4.1 Statistical Analysis of Surgically-Related Morphological Parameters of Proximal Human Femur (Study 1)

The first study provides a comprehensive overview of the surgically related morphological parameters. In Table 4 minimum, maximum, mean, standard deviation (STD), and median of the morphological parameters are shown. The highest STD was measured in NCHD, while the minimum STD was observed in NSA. Figure 8 illustrates the histograms showing the distribution of each parameter's diversity. OSA, OSH, TFL, NCVD have an acceptable normal distribution while NCDF, and NCDS are not normally distributed. Furthermore, the inter-correlation matrix, which states the Pearson's correlation between any two morphological parameters are calculated as shown in Table 5. The positive correlations represent a direct correlation where increasing one parameter causes the other parameter to increase. However, negative correlations denote an inverse correlation. Pearson's coefficient above 0.5 is considered as strong correlation. The strongest linear correlation was found between OSA and OSH, therefore a femur with a greater OSV also has a greater OSH. GTH and NSA as well as NCVD and OSA have the strongest inverse correlation (Pearson's coefficient of -0.62), thus an increase in NSA is associated with a decrease in the distance between FHC and great trochanter. Some parameters have no or very weak relation. For instance, NCDV and ATA have no definable relationship together as the Pearson's coefficient was measured as zero.

Table 4 - Statistical calculation (minimum, maximum, mean, standard deviation (STD), and median) of the morphological parameter.

Morphological Parameters	Min	Max	Mean ± STD	Median
FHD [mm]	37.95	54.35	46.29 ± 4.02	45.82
OSA [mm]	28.79	60.52	42.39 ± 5.98	42.61
OSV [mm]	38.73	68.46	54.37 ± 5.14	54.23
OSH [mm]	14.88	58.60	37.90 ± 6.95	38.16
ATA [°]	1.99	33.57	17.46 ± 6.77	18.45
NSA [°]	108.37	138.72	126.35 ± 4.29	126.81
GTH [mm]	-7.38	21.75	7.44 ± 5.06	6.95
TFL [mm]	364.80	517.93	439.22 ± 29.62	438.89
NCDF [mm]	0.01	6.45	1.51 ± 1.22	1.30
NCDS [mm]	0.06	8.41	2.42 ± 1.38	2.40
NCVD [mm]	-4.03	3.18	-0.09 ± 1.43	-0.01
NCHD [mm]	-3.75	9.52	2.17 ± 1.90	2.40

Table 5 – The inter-correlation matrix (p values) analyzed for the morphological parameters

Parameter	TFL	NCVD	GTH	NCDF	OSA	NCDS	OSH	NSA	ATA	NCHD	OSV
FHD	0.68	-0.29	0.08	0.20	0.29	0.07	0.27	0.11	-0.09	0.08	0.52
TFL		-0.03	-0.09	0.03	0.31	0.12	0.30	-0.05	-0.23	-0.03	0.75
NCVD			-0.55	-0.43	-0.62	0.27	-0.56	0.21	0.00	-0.05	0.25
GTH				0.38	0.39	-0.18	0.41	-0.62	-0.02	-0.04	-0.54
NCDF					0.26	0.03	0.25	-0.07	0.06	0.11	-0.10
OSA						-0.11	0.92	-0.45	-0.01	0.11	0.04
NCDS							0.10	0.07	-0.14	0.77	0.19
OSH								-0.49	-0.25	0.27	0.05
NSA									0.26	0.10	0.42
ATA										0.17	-0.13
NCHD											0.02
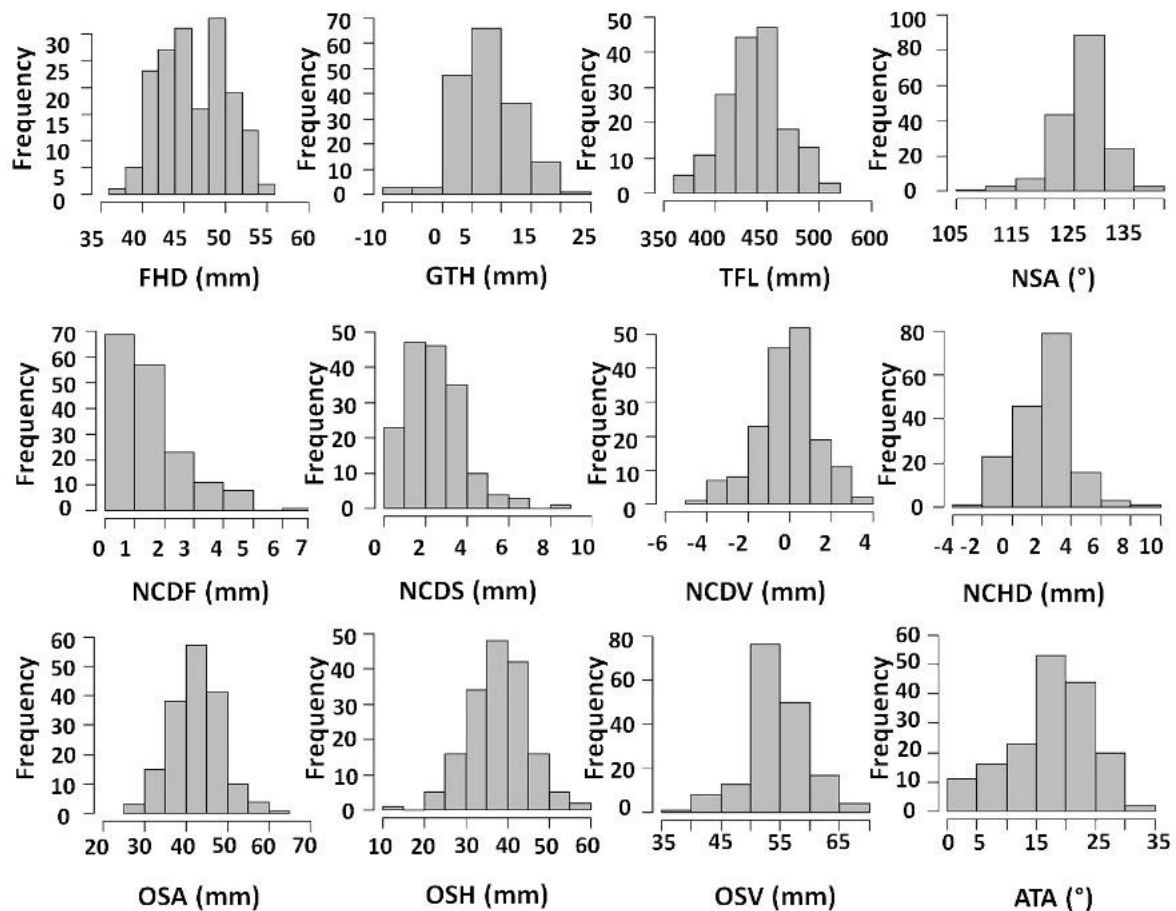
Figure 8 – Histograms of the morphological parameters showing their distribution as follows: a) FHD: Femoral head diameter. b) GTH: Greater trochanter height. c) TFL: Total femur length. d) NSA: Neck-Shaft angle. e) NCDF: Distance between the FHC and a plane parallel to the frontal plane containing the projection of the FHC to the FNA. f) NCDS: Distance between FHC and femoral neck axis (FNA) projected to the sagittal plane. g) NCVD: Vertical distance between the FHC and a plane parallel to transversal plane containing the projection of the FHC to the FNA. h) NCHD: distance between the FHC and a plane parallel to the frontal plane containing the projection of the FHC to the FNA. i) OSA: Absolute offset as the distance between femoral head centre (FHC) and femoral shaft axis. j) OSH: Horizontal offset as the projected distance between FHC and FSA to the frontal plane. k) OSV: Vertical offset as the vertical distance between FHC and the plane parallel to transversal plane containing the centre of the lesser trochanter. l) ATA: anteversion angle. All units are in mm except ATA and NSA which are in degree.

4.2 Accuracy Assessment of Image Based Surface Reconstructed Compared to Reference Optical 3D Scan (Study 2)

The average deviation values and Root Mean Square Error (RMSE) as a standard statistical metric are used for comparison and evaluation of simulation models performance (Willmott et al., 1985) to quantify the difference between the 9 image-based reconstructed models to the optical 3D scan (Table 6). The highest deviation was observed in "neck and greater trochanter" area with RMSE of 0.84. The negative values for the estimated percentage error of the surface areas represent the deviation of the underestimated areas and the positive values show the overestimated areas (Table 6). Figure 9 illustrates the estimated surface areas of all nine segmented models and the bone optical 3D scan. "Diaphysis" and "neck and greater trochanter" areas have the largest percentage errors of outer surface area with 2.92% and 2.57% respectively. As indicated in Figure 9 outer surface areas of the reconstructed models are not exceedingly different from the reference model.

Figure 10 illustrates the visual deviation using color-coded map to show the differences of each model compared to the bone optical 3D scan.

Table 6 - Average deviation of four different parts of femur.

Femur Region	Average Deviation Positive (mm)	Average Deviation Negative (mm)	Standard Deviation (mm)	RMSE (mm)	Average Percentage Errors of Surface Area (%)
Neck & Greater Trochanter Area	0.48	-0.72	0.78	0.84	-2.57
Proximal Metaphysis	0.61	-0.78	0.78	0.83	-2.06
Diaphysis	0.63	-0.18	0.41	0.69	2.92
Distal Metaphysis	0.66	-0.50	0.56	0.73	0.86
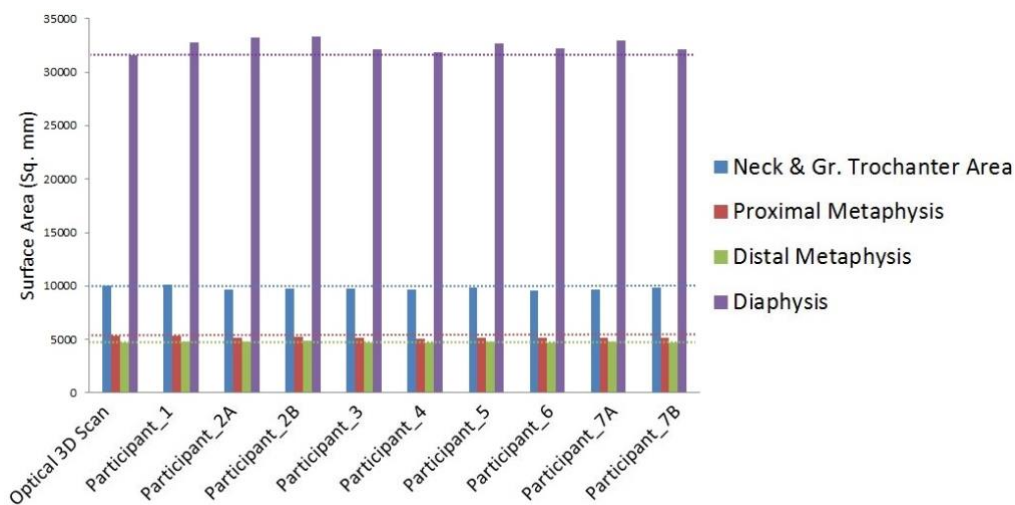
Figure 9 - Surface area of 4 segments (Neck and great trochanter area, proximal metaphysis, distal metaphysis and diaphysis) of the femur obtained from optical 3D scan (reference STL file) from 7 participating laboratories.
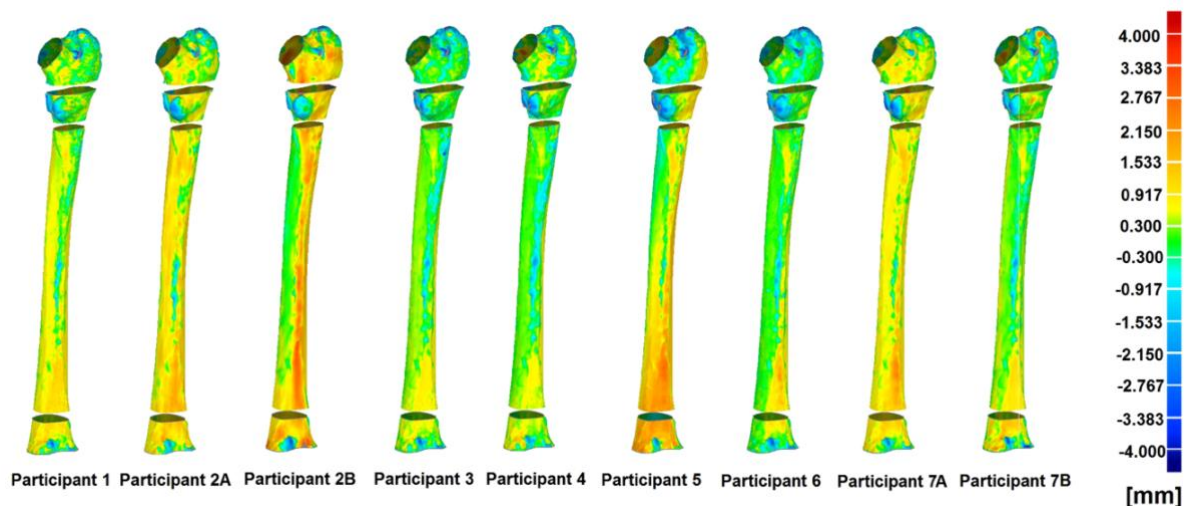
Figure 10- surface geometries comparison of 9 reconstructed models with the optical 3D scanned surface model. The red surface areas show overestimation of the reference model and blue areas indicate underestimation.

4.3   Comparison of the Finite Element Analysis with the Experiment Data (Study 3)

Figure 11 illustrates the strain measured by one of the strain gauges (strain gauge No.4) during the five repetition of the experiment. It proves that the experiment is repeatable without any drift signals. However, some drift signals were observed during the strain measurement of the other strain gauges. These drift signals were excluded for calculation of the average strain and STD.
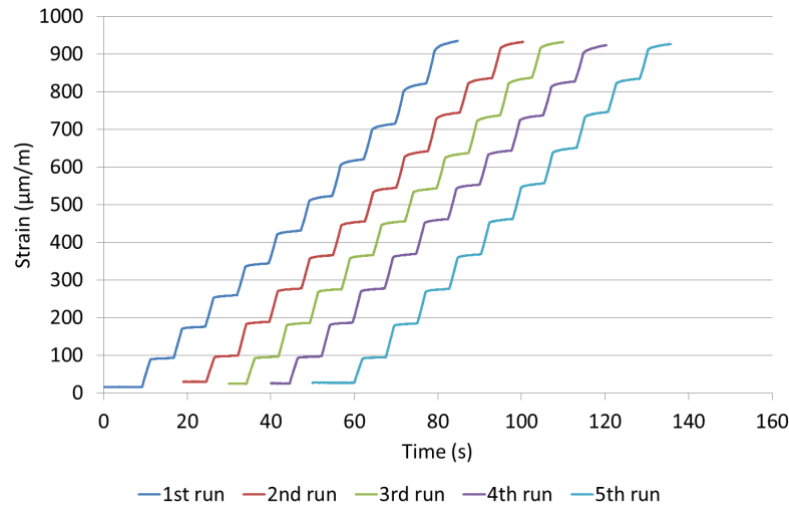
Figure 11 - The exemplary reproducibility of the five repeated experimental measurements at strain gauge 4 without drift of the signals. The timeline was adjusted for visibility.
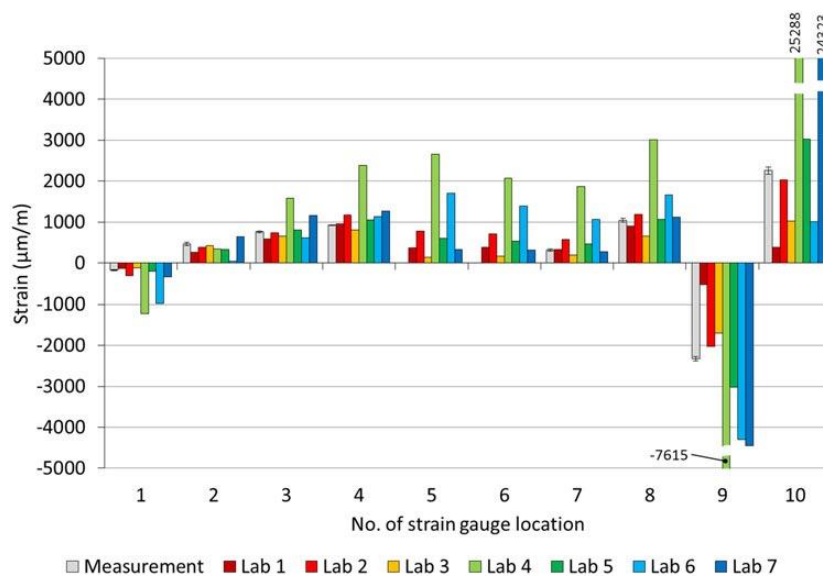
Figure 12 - The comparison of the calculated strains to the experimentally measured strains (+/- standard deviation) at 2.0 kN compression loading. Note that strain gauges 5 and 6 were ignored due to inaccurate measurements.

Following the evaluation of the measured strains at the maximum loading of 2kN, they were compared to the strains calculated by the FEA from the partnering laboratories of the round-robin test. The calculated strains by FEA from of all the seven partners are summarized in Figure 12 together with the experimentally measured strain values including the STD. The experimental values of strain gauges No.5 and No.6 were excluded as they were not

reproducible. Although the sign of strains (compression and tension) was correctly calculated nearly in all cases, the amount of strain varied considerably.

The FEA results of some laboratories were deviated less than 10 percent from the experiments while the obtained values of some other laboratories were ten times deviated from the experimental values. To compare the deviation of results obtained from FEA of each laboratory to the experimental result, a deviation percentage is calculated using Equation 3.

$$\delta_i = \left| \frac{\varepsilon_{cal_i} - \varepsilon_{exp_i}}{\varepsilon_{exp_i}} * 100\% \right|$$

Equation 3 – Deviation percentage

Where δ_i is the deviation percentage of the calculated strain ε_{cal_i} from the measured strain ε_{exp_i}. Index i is the number of the strain gauge location. The average of the percentage deviations with $i = \{1; 2; 3; 4; 7; 8; 9; 10\}$ per laboratory is shown in Figure 13. The FEA result of 4 laboratories showed an average accuracy of less than 40 % deviated from the experimentally calculated strains while the other 3 laboratories FEA result were deviated more than 120 % from the experimental result.
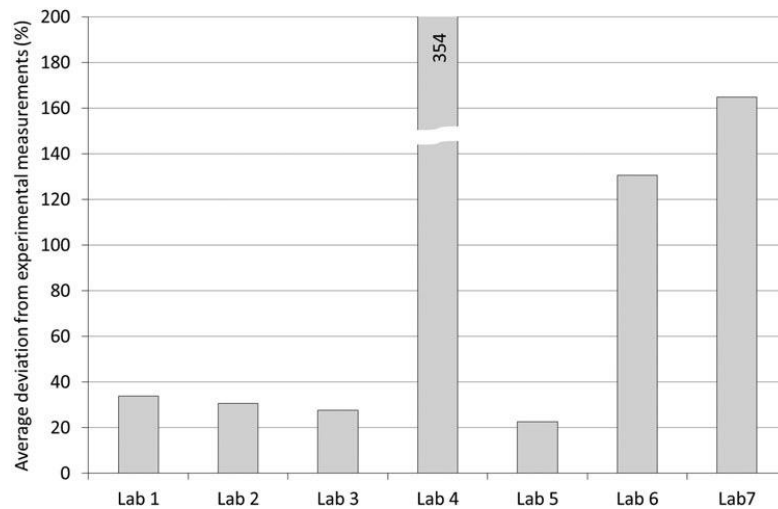
Figure 13 - The overview of the average deviation of the FEA results from the experimental measurements for all participating laboratories

Figure 14 shows the horizontal and vertical femoral head displacement under 2 kN. The grey bars represent the experimental results and other coloured bars illustrate the FEA results of all 7 laboratories. The calculated vertical displacements of femoral head by laboratories 1, 2, 3, and 5 were very similar to the experimental measurement while the result of laboratories 4 and 5 were higher than the experimental measurement. Moreover, the calculated vertical displacement for laboratory 6 was more than 8 times higher than the measured vertical displacement.
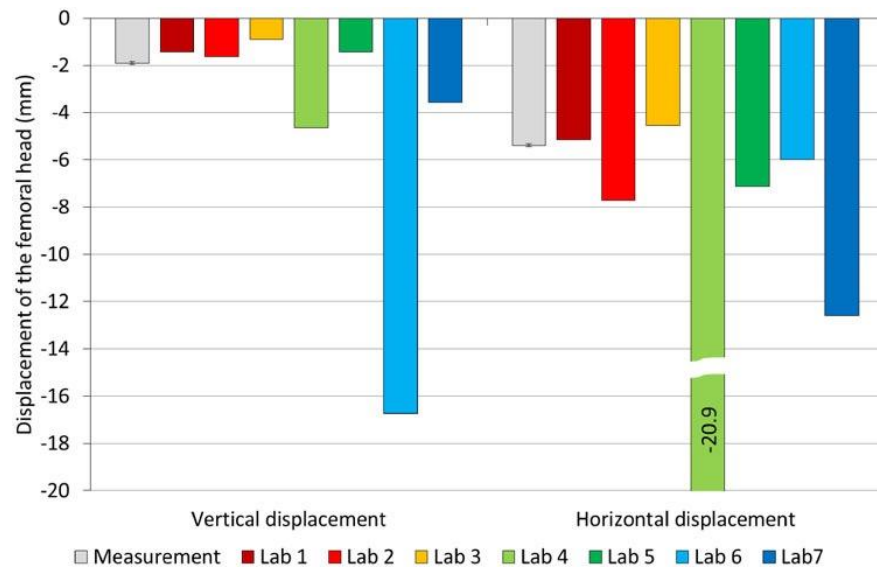
Figure 14 - Horizontal and vertical displacement of the femoral head at 2.0 kN load; the comparison between the measured displacement of the femoral head and the calculated displacement in FEA. Obtained results from FEA of laboratories 1,2,3, and 5 were closer to the experimental measurements.

5   Discussion

5.1   Surgical Relevance of Morphological Parameters of Proximal Human Femur (Study 1)

Femoral morphology is associated with pathology of diseases or incidence of fractures (Gnudi et al., 2012). Table 7 summarizes the clinical/biomechanical relevance of the parameters in endoprosthetics design and orthopaedic surgery planning.

Table 7 – Surgical and biomechanical relevance of proximal human femur's morphological parameters

Morphological Parameters	Clinical and Biomechanical relevance
FHD	Impingement /Prosthetics design/To deal with Cam-deformity
OSA	To design best-fit prosthetics/Restoration of physiological hip anatomy during total hip replacement (THR)
OSV	To design best-fit prosthetics
OSH	To design best-fit prosthetics
ATA	Preoperative planning of valgus/Varus derotational osteotomy of the proximal femur/To design best-fit prosthetics
NSA	Better predict hip fracture/Preoperative planning of valgus/Varus derotational osteotomy of the proximal femur
GTH	Restoration of physiological hip anatomy during THR
TFL	Better prediction of hip fracture
NCDF, NCDS, NCVD, NCHD	Impingement/Hip resurfacing

The findings of this study were compared to the similar performed studies on European population measuring femoral head diameter (FHD) (40 to 46.8mm) (Rubin et al., 1992). Very small FHD may cause impingement, dislocation or mechanical failure (Vo et al., 2015). Aberrancy of femoral head shape known as CAM-deformity is associated with dysmorphisms of the head-neck junction. The main reason for this is the fact that pre-epiphyseal fusion may be a censorious interval of vulnerability for development of morphologic abnormalities of the femoral head–neck junction. These dysmorphisms, mainly in young adults, should be therefore reconstructed to normal hip anatomy through surgical therapy (arthroscopic or mini-open surgery) to avoid the progression of osteoarthritis (Vo et al., 2015). These examples highlight the importance of considering FHD in biomedical and orthopaedic applications. Moreover, since joint ROM is also highly dependent on head size, FHD becomes essential for prosthetic design.

Femoral head offsets (OSA, OSH, and OSV) and anteversion angle (ATA) are required to design best-fit endoprosthetics to reduce the incidence of implant failure and loosening (Lecerf et al., 2009). Preoperative knowledge of femoral offset is also essential for total hip replacement (THR), because an accurate amount of femoral offset could improve hip abductor strength and enhance joint ROM, while simple restoration promises a reduced risk of wear, dislocation and failure (Lecerf et al., 2009). Since femoral offset is usually analysed on radiographs, we measured the OSH as a projection on the frontal plane to mimic this approach (37.90 ± 6.95mm). The OSA is a direct measurement of the length between head centre and FSA perpendicular to the axis of the femoral shaft (42.3±6.0mm). We measured a value of 54.4±4.1mm and 7.44±5.1mm for OSV and GTH respectively. However, OSV and GTH are poorly presented in the literature. Both OSV and GTH are relevant for restoration of physiological hip anatomy during THR. In most implant designs, a decrease in the off-set

results in an increased instability, which is often counterbalanced using long neck femoral heads. ATA was determined to be 17.5±6.7° in this study. However, ATA reported in the literature largely varies from 10.4-24.7° (mean value) in European samples (Ollivier et al., 2015). Presumably, this occurs due to different definitions of the axes. Significant variations have also been reported for ATA in right and left hip (Kingsley and Olmsted, 1948). However, a satisfactory explanation for this parameter is still missing. Changes in ATA during childhood play an important role in the physiological development of the hip joint. Malrotation of ATA after intramedullary nailing can cause joint pain, leading to movement limitations, which therefore disturbs the patient's daily life. Acceptable preoperative determination of ATA can be directly related to patient's satisfaction after surgery. ATA is also associated with lower-extremity disorders such as in-/out-toeing (Srimathi et al., 2012), impingement and osteoarthritis (Tonnis and Heinecke, 1999). Degenerative diseases of the hip or the knee can accordingly be developed by malrotation. All these brighten the importance of proper orientation of the femoral component in THR to avoid dysfunction.

Adequate estimation of NSA and TFL can help to better predict hip fracture (Gregory and Aspden, 2008). The osteotomies of the pelvis and upper femur in surgical management of developmental dysplasia of the hip are very beneficial and enduring. Intertrochanteric osteotomies were replaced by periacetabular osteotomies for treatment of most dysplasia-related conditions (Santore et al., 2006). NSA and ATA are important parameters required for preoperative planning of valgus or varus derotational osteotomy of the proximal femur. Valgus osteotomy can be sometimes useful to maintain or increase congruency of the hip joint, while varus osteotomy may play a role in optimizing the joint space. A higher NSA is in relation to the incidence of femoral neck fractures (Gnudi et al., 2012), particularly in osteoporotic patients (Esenyel et al., 2011). A 10° valgus placement of the femoral component can protect against spontaneous fractures of the femoral neck in healthy bone (Schnurr et al., 2009), which underlines the importance of preoperative determination of NSA. The effectiveness of valgus osteotomy (increased NSA) for femoral neck non-union is unquestioned. Limb-length discrepancy, malrotations and posttraumatic deformities can benefit from intertrochanteric osteotomy. Grade II slipped capital femoral epiphysis, Legg-Calvé-Perthes disease, and osteonecrosis can sometimes be effectively treated with intertrochanteric osteotomy. Therefore, femoral osteotomies should be thoroughly planned and performed with respect to the possible need for future conversion to total hip replacement.

The parameters NCVD, NCHD, NCDS, and NCDF in addition to FHD play a key role in impingement problems (Lindsey and Krieg, 2011). An adverse relationship between the femoral component size and the neck diameter was found to be a reason for a higher risk of dislocation. Subject to the fact that the femoral component is inserted with strict respect to implantation guidelines, its position should also be in line with the femoral neck axis (FNA). However, coxal anatomy often reveals an off-set of the femoral head centre (NCVD, NCHD, NCDS and NCDF) which may have an adverse impact on hip resurfacement dislocation. In this study, a relationship between coxa valga/vara and the position of the femoral head centre as well as a relationship between anteversion of the neck and position of the femoral head centre is revealed. These will initially help orthopaedic surgeons to minimize the risk of dislocation in preoperative planning of THR.

5.2 *Accuracy and Reliability of Image-Based 3D reconstruction of Human Bones in Orthopaedic Biomechanics (Study 2)*

Finite element models are widely used based on specific geometrical characteristics extracted from medical imaging data. This study presents a deviation analysis to evaluate different segmentation methods based on CT scan compared to optical 3D surface scan of the same

bone. Thereby, the reconstruction results of seven different biomechanics laboratories were compared to evaluate how human skills, methods of segmentation, and different software packages can cause imprecision in image-based reconstructed models.

This study investigated a variety of conditions, which may have influenced the accuracy of the segmentation process. The segmentations of "neck and greater trochanter" area and "proximal metaphysis" areas showed the greatest deviations with RMSE of 0.84mm and 0.83mm respectively (Table 6). Thevenot et al. (2014) reported the accuracy of a novel method for automatically reconstructed 3D model from 2D hip radiograph, and Verim et al. (2013) evaluated the reconstructed proximal femur from different images of different devices. They both found that the greatest error occurred in the trochanter area which is in a good agreement with the result of this study. Väänänen et al. (2011) assessed the 3D shape of proximal femur using two different methods; shape template and bone mineral density image. They also found out that the maximum discrepancies exist in trochanter area, ranging from 0.7 to 2.6mm. The results of this study also showed the similar range of discrepancies. Schumann et al. (2010) used clinically relevant morphometric parameters measurement of the proximal femur to examine the accuracy of their reconstructed method. In their study, the highest average deviations were also observed in trochanter area. Rathnayaka et al. (2012) conducted a study to compare the accuracy of MRI and CT reconstructed 3D models where they also estimated the highest deviations was observed in the "neck and greater trochanter" region. The highest deviations, usually observed in the "neck and greater trochanter" area, are probably due to geometrical complications exist in this area. In the current study, the highest estimated discrepancy from the reconstructed models is 0.79mm. The previous studies of Gelaude et al. (2006), (Gelaude et al., 2008) on accuracy assessment of reconstructed models based on medical images, suggest that the mean 3D deviation of reconstructed models should be in the range of 1mm. Since clinical hip fractures commonly occur in the neck area (Thevenot et al., 2014), more accuracy in reconstruction of this area is required to have more precise FE analysis results. Furthermore, as observed in Figure 9, there was no outlier in the accuracy assessment comparison, and all reconstructed 3D models have similar range of deviations. However, if peak discrepancies are observed, they can simply be disregarded because they are local. The outer surface areas of the reconstructed models providing the surface meshes for FE analysis were also estimated in this study. Highest errors of the outer surface area were observed in "diaphysis" and "neck and greater trochanter" regions as shown in Figure 10 using color-coded map to illustrate that "diaphysis" and "neck and greater trochanter" regions have the highest surface discrepancies compared to the real bone 3D optical scan. Therefore, these two regions are the most critical regions for reconstruction of 3D models based on medical images and should carefully be processed. The results also suggest that the quality of the image segmentation is rather independent of reconstruction processing software. The differences observed in segmentation times can be associated with either individual investigator speed of segmentation or the usability of the software.

5.3 *Numerical Calculation versus Experimental Measurement in Orthopaedic Biomechanics (Study 3)*

The present work is a round-robin study involving seven participating laboratories to compare the results of the FE analyses on the human femur with a common experimental setup as the ground truth. It has turned out that there are partially very high deviations between the experimentally determined and numerically calculated results. While four laboratories achieved an average deviation of less than 40%, the deviations averaged more than 120% in three other laboratories. Therefore, it can be concluded that despite decades of experience, the FEA of the human femur has not yet reached the standard and precision sought by the

biomechanical research community. A round-robin FEA such as the one conducted here has already been suggested by Helgason et al. (2008). However, no such study has been documented in the scientific literature so far. Consequently, to our knowledge, this is the first *in silico* benchmark study with so many different participating laboratories undertaken to highlight the differences in the FE modeling of the human femur in terms of strain and displacement calculation. To the best knowledge of the author, the only similar study was carried out by two laboratories, whereby one conducted the experimental tests, and the other conducted the FE calculations in a double-blinded manner (Trabelsi et al., 2011). Using a mechanical setup comparable to our approach with n=12 human femur specimens, the mean of absolute deviations between the calculated strains and measured strains was 22%.

An outstanding strength of this study is that several national and international centres and the researchers conducting the FE analyses did not know the experimental results in advance. That is why this study is considered as a prospective approach. Dreischarf et al. (2014) compared the result of eight published study on the FEA of the lumbar spine, hence in a retrospective and non-blinded way.

In this study, different elasticity-density relationships were used by the different laboratories, which influenced the strain calculations. Therefore, individual deviations probably resulted from the different material laws used. Schileo et al. (2007) showed in a computational study that the use of different density-dependent material laws has an enormous effect on the strain calculation. In contrast to the isotropic material definition used in the current study, Peng et al. (2006) showed a very small deviation in the mechanical response when using anisotropic material behaviour. Besides, material laws and their corresponding data, and the mapping strategy also influences the numerical results as shown by Helgason et al. (2016) using five different material mapping methods. Furthermore, the strategy of material data assignment (node- or element-wise) will have a significant impact on the numerical results (Chen et al., 2015).

In conclusion, the first part of this dissertation evidently reports important morphological parameters of the proximal human femur in physiological range to establish a database for orthopaedic and biomedical research purposes. The knowledge on the parameters distributions and correlations provide a key tool for further studies, which can contribute to a prolonged lifetime of load-bearing joint replacements, and reduce the incidence of micro-motion, impingement, loosening, and periprosthetic fracture.

The second part of this work shows that the average deviation of CT based models prepared by experts with different skills using various software packages from a bone surface scan is very low. This reveals that the effect of human expertise and use of different software packages and corresponding methodologies have a negligible effect on the accuracy of the reconstruction procedure from medical images. Therefore, image-based reconstructed models are reliable to be employed in FE models for clinical applications.

Study 3 provides sufficient evidence that that the computational analysis of long bones still has to be improved. Therefore, further research should be performed on the accuracy and reliability assessment of the computational modelling. The main outcome of this part of the study was to underline that even if the power of computational modelling is largely increasing, the accuracy of FEA modelling in biomechanics is a challenge specifically for the clinical purposes. Despite the presented results, FEA is an important tool for the biomechanical analysis as shown in valuable clinical studies based on imaged-based FEA (Yosibash et al. 2014; Sternheim et al. 2018). On this basis, it can be concluded that carefully performance of material mapping, meshing of geometry, and more importantly the definition of relationship between grey-scale values, density and stiffness can highly improve the accuracy of the results.

6 Future Works

The work performed provides basis for future research in several areas. Many different adaptations, tests, and experiments have been left for the future. The following three research questions are the areas, which require further investigations:

- **Morphological study**

The relevance of proximal femur for orthopaedic diseases such as impingement, valgus/varus derotational, and designing the best fit for total hip endoprostheses were thoroughly investigated in this study. Since pelvic bone is another component of the hip joint, the same morphological study should be performed on characterization of human pelvis based on the CT images. More specifically, acetabulum plays an important role in designing THR and diseases such as impingement. Therefore, surgical and clinical relevance of human pelvis should be also investigated and an appropriate population-based detailed database is required for orthopaedics and biomechanical research aspects.

- **Accuracy Assessment of Computational Work after Implantation of Total Hip Replacement**

A more complicated geometry could result into more deviations. An accuracy assessment of image-based modelling using computer aided design technics (CAD) is lacking in the field of orthopaedic biomechanics. Furthermore, there are many factors in such a complex FEA model including defining the contacts of endoprosthetics and bone, assigning material properties, defining boundary conditions, which need to be assessed by comparing with the experimental results.

Furthermore, the femur used in this study can be further implanted by total hip replacement and additional experimental strain measurements under the defined load can be also performed. In that case, another struggle will be taken into account, i.e., the contact between implant and bone. For an uncemented total hip replacement, assumptions must be made considering the type of contact, friction behaviour and in the case of press-fit implantation, pre-stress should be considered in the surrounding bone.

- **Periprosthetic Bone Fracture Biomechanics Following Total Hip Replacement: Computational Analysis and Experimental Validation**

Computational and experimental characterization of periprosthetic fraction happening in the hip joint after total hip replacement would provide a very comprehensive overview for the clinicians and biomechanical engineers. Bone fracture in the vicinity of total joint replacement components is commonly called periprosthetic fracture (PPF). PPF should be analysed after low-impact energy accidents such as stumbling and sideway fall. Developing a reliable validated finite element (FE) model with proper material properties and boundary conditions in order to predicting the risk of PPF will be an interesting challenge as a future work. A FE model of the compound of total hip replacement and adjacent bone stock which provides should be developed to investigate bone fracture in the vicinity the of hip joint endoprosthesis by implementing knowledge of mechanical engineering, material engineering and biomechanics and orthopaedics. The proposed approach will provide a reliable validated FE model to simulate and predict fracture risk of bone in the proximity of hip joint prosthetic. It allows orthopaedic surgeons to have a better overview of the fracture risk factors from mechanical point of view and also enhance engineers to design a superior total joint endoprostheses.

7 Summary

Comprehending of the patients' native bone morphology including the variations and correlations is essential in orthopaedic surgery to perform precise pre-operative planning and surgery as well as to appropriately design optimal medical implants. Thus, more population-based detailed databases of the bone morphology are necessary. The aim of the present work is to provide a comprehensive database of surgically relevant morphological landmarks of human proximal femur, and the accuracy assessment of 3D reconstructed morphology based on medical images as well as numerical analysis in relevant anatomical landmarks of the human femur. Twelve morphological parameters of the femur in 169 healthy human subjects were investigated through evaluation of 3D-reconstructed CT scans. The Pearson's coefficients of correlations were calculated using a statistical t-test method for each pair of parameters. Seven research groups then reconstructed nine 3D models of one human femur based on a computer tomography image using their own computational methods. As a reference model for accuracy assessment, a 3D surface scan of the human femur was created using an optical measuring system. Prior to comparison, the femur was divided into four areas; "neck and greater trochanter", "proximal metaphysis", "diaphysis", and "distal metaphysis". The deviation analysis was carried out in GEOMAGIC studio v.2013 software. A native human femur was prepared for a compression test in a testing machine measuring the strains at 10 bone locations as well as the deformation of the bone in terms of the displacement of the loading point at a load of 2kN. The computed tomography data of the bone with a calibration phantom as well as the orientation of the bone in the testing machine with the according boundary conditions were delivered to seven participating laboratories. In addition, the location and direction of the strain gauges were communicated. The laboratories were asked to perform a finite element analysis simulating the experimental setup and deliver their results (strains and deformation) to the coordinator of the study with no access or knowledge to the experimental results.

In conclusion, in first study, as an advantage towards previous studies, an extensive set of proximal femoral morphology parameters with a statistically standardized method was investigated to expand the existing knowledge. The results of first study (publication 1) provide a key tool for further studies, which can contribute to a prolonged lifetime of load-bearing joint replacements by reduction of the incidence of micro-motion, impingement, loosening, and periprosthetic fracture.

The results of second study (publication 2) revealed that the highest deviation errors in 3D reconstruction of human femur occurred in "neck and greater trochanter" area and "proximal metaphysis" area with RMSE of 0.84mm and 0.83mm respectively. It shows that the average deviation of reconstructed models prepared by experts with various methods, skills and software from the surface 3D scan was lower than 0.79mm, which was not a significant discrepancy. In the third study (publication 3), it was observed that four laboratories had deviations from the experimentally measured strains of less than 40%, and three laboratories had deviations of their numerically determined values compared to the experimental data of more than 120%. These deviations are thought to be based on different material laws and material data, as well as different material mapping methods. Further investigations should be conducted to clarify and assess the reasons for the large deviations observed in the numerical data. Hence, enhanced precision and reproducibility of finite element modelling of the human femur is a challenging task for future studies.

These presented studies attempted to highlight the importance of human femur morphology on biomechanically-related surgical procedures and the required accuracy of image-based biomechanical analysis in the field of orthopaedic biomechanics.

8 Zusammenfassung

Das Verständnis der nativen Knochenmorphologie der Patienten einschließlich der Variationen und Korrelationen ist in der Orthopädischen Chirurgie unerlässlich, um eine exakte präoperative Planung und Operation durchführen und entsprechend Implantate optimal gestalten zu können. Daher sind mehr bevölkerungsbezogene Datenbanken der Knochenmorphologie notwendig. Das Ziel der vorliegenden Arbeit ist es, eine umfassende Datenbank mit chirurgisch relevanten morphologischen Landmarken des menschlichen proximalen Femurs sowie einer Genauigkeitsbewertung der 3D rekonstruierten Morphologie bereitzustellen. Diese basieren auf medizinischen Bilddaten sowie der numerischen Analyse relevanter anatomischer Landmarken des humanen Femurs. Zwölf morphologische Parameter des Femurs wurden durch die Auswertung von 3D-rekonstruierten CT-Scans von 169 gesunden Probanden untersucht. Die Pearson-Korrelationskoeffizienten wurden mit Hilfe einer statistischen t-Testmethode für jedes Parameterpaar berechnet. Sieben Arbeitsgruppen rekonstruierten anschließend neun virtuelle 3D-Modelle eines humanen Oberschenkelknochens auf der Grundlage eines Computertomographie-Scans mit eigenen Berechnungsmethoden. Als Referenzmodell für die Genauigkeitsbeurteilung wurde mit einem optischen Messsystem ein 3D-Oberflächenscan des realen humanen Oberschenkelknochens erstellt. Vor dem Vergleich wurde der Oberschenkelknochen in vier Bereiche unterteilt: "Hals und Trochanter", "proximale Metaphyse", "Diaphyse" und "distale Metaphyse". Die Abweichungsanalyse wurde in der Software GEOMAGIC studio v.2013 durchgeführt. Für einen Druckversuch in einer Universalprüfmaschine wurde ein nativer humaner Femur vorbereitet, der die Dehnungen an 10 Knochenstellen sowie die Verformung des Knochens im Hinblick auf die Verschiebung der Belastungsstelle bei einer Belastung von 2 kN misst. Die Computertomographie-Daten des Knochens, welche ein Kalibrierungsphantom sowie die Ausrichtung des Knochens in der Prüfmaschine mit den entsprechenden Randbedingungen enthielten, wurden sieben teilnehmende Labore bereitgestellt. Darüber hinaus wurden die Lage und Richtung der Dehnungsmessstreifen mitgeteilt. Die Teilnehmer wurden gebeten eine Finite-Elemente-Analyse durchzuführen, die den Versuchsaufbau simuliert. Die Ergebnisse (Dehnungen und Verformungen) wurden dem Koordinator der Studie zur Verfügung gestellt, wobei die Teilnehmer weder Zugriff auf der Versuchsergebnisse noch Kenntnis davon hatten. Zusammenfassend lässt sich sagen, dass in der ersten Studie im Vergleich zu früheren Studien ein sehr umfangreicher Satz von Morphologieparametern der proximalen Femora mit einer statistisch standardisierten Methode untersucht wurde. Die Ergebnisse der ersten Studie (Publikation 1) sind ein wichtiger Grundstein für weitere Studien, die zu einer verlängerten Lebensdauer des last-tragenden Gelenkersatzes durch verringertes Auftreten von Mikrobewegungen, Impingement, Lockerungen und periprothetischen Frakturen beitragen können.

Die Ergebnisse der zweiten Studie (Publikation 2) zeigten, dass die größten Abweichungen im Bereich "Hals und größerer Trochanter" und "proximale Metaphyse" mit RMSE von 0,84 mm bzw. 0,83 mm auftraten. Abschließend zeigte sich, dass die mittlere Abweichung der rekonstruierten Modelle, welche von Experten mit verschiedenen Methoden, Fähigkeiten und Software vom 3D-Oberflächenscan abgeleitet wurden, niedriger als 0,79 mm ist und sich nicht signifikant unterscheidet. In der dritten Studie (Publikation 3) wurde beobachtet, dass vier Teilnehmer Abweichungen von den experimentell gemessenen Stämmen von weniger als 40% von gegenüber den experimentell gemessenen Stämmen aufwiesen. Weiterhin wiesen die numerisch bestimmten Werte dreier Laboratorien Abweichungen von mehr als 120% gegenüber den experimentellen Daten auf. Es wird davon ausgegangen, dass diese Abweichungen auf unterschiedlich gewählten Materialgesetzen und Materialdaten sowie auf

unterschiedlichen Materialabbildungsmethoden beruhen. Weitere Untersuchungen sind geplant, um die Ursachen für die großen Abweichungen in den numerischen Daten zu klären und zu bewerten. Daher stellt die Präzision und die Reproduzierbarkeit von Finite-Elemente-Modellierungen des humanen Oberschenkelknochens eine herausfordernde Aufgabe in zukünftigen Studien dar.

Die vorgelegten Studien verdeutlichen die Bedeutung der menschlichen Oberschenkelknochen-Morphologie für chirurgische Verfahren mit biomechanischer Relevanz und heben die notwendige Genauigkeit der bildbasierten biomechanischen Analyse im Bereich der orthopädischen Biomechanik hervor.

9   References

3D4MEDICAL.COM. 2014. *Essential Skeleton, Mac OS versions, Version 4* [Online]. 3D4Medical.com, LLC. [Accessed].

AHMADY, A., SOODMAND, E., SOODMAND, I. & MILANI, T. L. 2014. The effect of various heights of high-heeled shoes on foot arch deformation: Finite element analysis. *Journal of Foot and Ankle Research,* 7**,** A78.

ARUN, K. & JADHAV, K. 2016. Behaviour of human femur bone under bending and impact loads. *Eur. J. Clin. Biomed. Sci,* 2**,** 6-13.

BAGWELL, J. J., SNIBBE, J., GERHARDT, M. & POWERS, C. M. 2016. Hip kinematics and kinetics in persons with and without cam femoroacetabular impingement during a deep squat task. *Clin Biomech (Bristol, Avon),* 31**,** 87-92.

BAHARUDDIN, M. Y., SALLEH, S.-H., ZULKIFLY, A. H., LEE, M. H. & MOHD NOOR, A. 2014. Morphological study of the newly designed cementless femoral stem. *BioMed research international,* 2014**,** 692328-692328.

BASSO, T., KLAKSVIK, J., SYVERSEN, U. & FOSS, O. A. 2012. Biomechanical femoral neck fracture experiments--a narrative review. *Injury,* 43**,** 1633-9.

BECK, M., KALHOR, M., LEUNIG, M. & GANZ, R. 2005. Hip morphology influences the pattern of damage to the acetabular cartilage: femoroacetabular impingement as a cause of early osteoarthritis of the hip. *J Bone Joint Surg Br,* 87**,** 1012-8.

BEHRENS, B.-A., NOLTE, I., WEFSTAEDT, P., STUKENBORG-COLSMAN, C. & BOUGUECHA, A. 2009. Numerical investigations on the strain-adaptive bone remodelling in the periprosthetic femur: Influence of the boundary conditions. *BioMedical Engineering OnLine,* 8**,** 7.

BRUCEBLAUS.COM 2014. Medical gallery of Blausen Medical 2014. *Wikiversity Journal of Medicine* 1**,** 10.

CATTANEO, P. M., DALSTRA, M. & FRICH, L. H. 2001. A three-dimensional finite element model from computed tomography data: A semi-automated method. *Proceedings of the Institution of Mechanical Engineers, Part H: Journal of Engineering in Medicine,* 215**,** 203-212.

CHEN, G., WU, F. Y., LIU, Z. C., YANG, K. & CUI, F. 2015. Comparisons of node-based and element-based approaches of assigning bone material properties onto subject-specific finite element models. *Med Eng Phys,* 37**,** 808-12.

CHOI, J. Y., CHOI, J. H., KIM, N. K., KIM, Y., LEE, J. K., KIM, M. K., LEE, J. H. & KIM, M. J. 2002. Analysis of errors in medical rapid prototyping models. *International Journal of Oral and Maxillofacial Surgery,* 31**,** 23-32.

CHU, C., CHEN, C., LIU, L. & ZHENG, G. 2015. FACTS: Fully Automatic CT Segmentation of a Hip Joint. *Ann Biomed Eng,* 43**,** 1247-59.

CLEMENT, N. D., S PATRICK-PATEL, R., MACDONALD, D. & BREUSCH, S. J. 2016. Total hip replacement: increasing femoral offset improves functional outcome. *Archives of orthopaedic and trauma surgery,* 136**,** 1317-1323.

CONG, A., BUIJS, J. O. & DRAGOMIR-DAESCU, D. 2011. In situ parameter identification of optimal density-elastic modulus relationships in subject-specific finite element models of the proximal femur. *Med Eng Phys,* 33**,** 164-73.

CROOIJMANS, H. J. A., LAUMEN, A. M. R. P., VAN PUL, C. & VAN MOURIK, J. B. A. 2009. A new digital preoperative planning method for total hip arthroplasties. *Clinical orthopaedics and related research,* 467**,** 909-916.

DREISCHARF, M., ZANDER, T., SHIRAZI-ADL, A., PUTTLITZ, C. M., ADAM, C. J., CHEN, C. S., GOEL, V. K., KIAPOUR, A., KIM, Y. H., LABUS, K. M., LITTLE, J. P., PARK, W. M., WANG, Y. H., WILKE, H. J., ROHLMANN, A. & SCHMIDT, H. 2014. Comparison of eight published static finite element models of the intact lumbar spine: predictive power of models improves when combined together. *J Biomech,* 47**,** 1757-66.

EBERLE, S., GOTTLINGER, M. & AUGAT, P. 2013. An investigation to determine if a single validated density-elasticity relationship can be used for subject specific finite element analyses of human long bones. *Med Eng Phys,* 35**,** 875-83.

References

ECKSTEIN, F., CHARLES, H. C., BUCK, R. J., KRAUS, V. B., REMMERS, A. E., HUDELMAIER, M., WIRTH, W. & EVELHOCH, J. L. 2005. Accuracy and precision of quantitative assessment of cartilage morphology by magnetic resonance imaging at 3.0T. *Arthritis Rheum,* 52**,** 3132-6.

ESENYEL, M., OZEN, A., ESENYEL, C. Z., REZVANI, A., SARIYILDIZ, M. A. & ERGIN, O. 2011. Hip structural changes and fracture risk in osteopenia and osteoporosis. *Eurasian J Med,* 43**,** 73-8.

FAN, X., CHEN, Z., JIN, Z., ZHANG, Q., ZHANG, X. & PENG, Y. 2018. Parametric study of patient-specific femoral locking plates based on a combined musculoskeletal multibody dynamics and finite element modeling. *Proc Inst Mech Eng H,* 232**,** 114-126.

FITZWATER, K. L., MARCELLIN-LITTLE, D. J., HARRYSSON, O. L., OSBORNE, J. A. & POINDEXTER, E. C. 2011. Evaluation of the effect of computed tomography scan protocols and freeform fabrication methods on bone biomodel accuracy. *Am J Vet Res,* 72**,** 1178-85.

FRIESE, K.-I., BLANKE, P. & WOLTER, F.-E. 2011. YaDiV—an open platform for 3D visualization and 3D segmentation of medical data. *The Visual Computer,* 27**,** 129-139.

GELAUDE, F., VANDER SLOTEN, J. & LAUWERS, B. 2006. Semi-automated segmentation and visualisation of outer bone cortex from medical images. *Comput Methods Biomech Biomed Engin,* 9**,** 65-77.

GELAUDE, F., VANDER SLOTEN, J. & LAUWERS, B. 2008. Accuracy assessment of CT-based outer surface femur meshes. *Comput Aided Surg,* 13**,** 188-99.

GNUDI, S., SITTA, E. & PIGNOTTI, E. 2012. Prediction of incident hip fracture by femoral neck bone mineral density and neck-shaft angle: a 5-year longitudinal study in post-menopausal females. *Br J Radiol,* 85**,** e467-73.

GREGORY, J. S. & ASPDEN, R. M. 2008. Femoral geometry as a risk factor for osteoporotic hip fracture in men and women. *Med Eng Phys,* 30**,** 1275-86.

GULLBERG, B., JOHNELL, O. & KANIS, J. A. 1997. World-wide projections for hip fracture. *Osteoporos Int,* 7**,** 407-13.

HAMBLI, R., BETTAMER, A. & ALLAOUI, S. 2012. Finite element prediction of proximal femur fracture pattern based on orthotropic behaviour law coupled to quasi-brittle damage. *Med Eng Phys,* 34**,** 202-10.

HELGASON, B., GILCHRIST, S., ARIZA, O., VOGT, P., ENNS-BRAY, W., WIDMER, R. P., FITZE, T., PÁLSSON, H., PAUCHARD, Y., GUY, P., FERGUSON, S. J. & CRIPTON, P. A. 2016. The influence of the modulus–density relationship and the material mapping method on the simulated mechanical response of the proximal femur in side-ways fall loading configuration. *Medical Engineering & Physics,* 38**,** 679-689.

HELGASON, B., PERILLI, E., SCHILEO, E., TADDEI, F., BRYNJOLFSSON, S. & VICECONTI, M. 2008. Mathematical relationships between bone density and mechanical properties: a literature review. *Clin Biomech (Bristol, Avon),* 23**,** 135-46.

JACK, C. M., WALTER, W. L., SHIMMIN, A. J., CASHMAN, K. & DE STEIGER, R. N. 2013. Large diameter metal on metal articulations. Comparison of total hip arthroplasty and hip resurfacing arthroplasty. *J Arthroplasty,* 28**,** 650-3.

JENSEN, R. K. 1993. Human Morphology: Its role in the mechanics of movement. *Journal of Biomechanics,* 26**,** 81-94.

KANG, S. H., KIM, M. K., KIM, H. J., ZHENGGUO, P. & LEE, S. H. 2014. Accuracy assessment of image-based surface meshing for volumetric computed tomography images in the craniofacial region. *J Craniofac Surg,* 25**,** 2051-5.

KHALEEL, N. & SHAIK, H. S. 2014. Osteometric study of human femur. *International Journal of Research in Medical Sciences,* 2**,** 104.

KINGSLEY, P. C. & OLMSTED, K. L. 1948. A study to determine the angle of anteversion of the neck of the femur. *J Bone Joint Surg Am,* 30a**,** 745-51.

KLUESS, D. 2010. Finite element analysis in orthopaedic biomechanics. *Finite element analysis.* IntechOpen.

KLUESS, D., MARTIN, H., MITTELMEIER, W., SCHMITZ, K. P. & BADER, R. 2007. Influence of femoral head size on impingement, dislocation and stress distribution in total hip replacement. *Med Eng Phys,* 29**,** 465-71.

References

KLUESS, D., SCHULTZE, C., LUBOMIERSKI, A., MITTELMEIER, W., SCHMITZ, K.-P. & BADER, R. 2008. Finite-element-analysis of a cemented ceramic knee arthroplasty under worst case scenarios. *Journal of Biomechanics*, S237.

KLUESS, D., SOUFFRANT, R., MITTELMEIER, W., WREE, A., SCHMITZ, K. P. & BADER, R. 2009. A convenient approach for finite-element-analyses of orthopaedic implants in bone contact: modeling and experimental validation. *Comput Methods Programs Biomed,* 95, 23-30.

LABRONICI, P. J., DE OLIVEIRA CASTRO, G. N. P., NETO, S. R., GOMES, H. C., HOFFMANN, R., DE AZEVEDO NETO, J. N., FRANCO, J. S., DE NORONHA ROCHA, T. H. & ALVES, S. D. 2015. FEMORAL ANTEVERSION AND THE NECK-SHAFT ANGLE: RELATIONSHIP WITH HIP OSTEOARTHRITIS. *Revista brasileira de ortopedia,* 46, 69-74.

LALONE, E. A., WILLING, R. T., SHANNON, H. L., KING, G. J. & JOHNSON, J. A. 2015. Accuracy assessment of 3D bone reconstructions using CT: an intro comparison. *Med Eng Phys,* 37, 729-38.

LECERF, G., FESSY, M. H., PHILIPPOT, R., MASSIN, P., GIRAUD, F., FLECHER, X., GIRARD, J., MERTL, P., MARCHETTI, E. & STINDEL, E. 2009. Femoral offset: anatomical concept, definition, assessment, implications for preoperative templating and hip arthroplasty. *Orthop Traumatol Surg Res,* 95, 210-9.

LI, H., WANG, Y., ONI, J. K., QU, X., LI, T., ZENG, Y., LIU, F. & ZHU, Z. 2014. The role of femoral neck anteversion in the development of osteoarthritis in dysplastic hips. *Bone Joint J,* 96-b, 1586-93.

LINDSEY, J. D. & KRIEG, J. C. 2011. Femoral malrotation following intramedullary nail fixation. *J Am Acad Orthop Surg,* 19, 17-26.

LITTLE, J. P., TADDEI, F., VICECONTI, M., MURRAY, D. W. & GILL, H. S. 2007. Changes in femur stress after hip resurfacing arthroplasty: Response to physiological loads. *Clinical Biomechanics,* 22, 440-448.

MALIK, A., MAHESHWARI, A. & DORR, L. D. 2007. Impingement with total hip replacement. *J Bone Joint Surg Am,* 89, 1832-42.

OKA, K., MURASE, T., MORITOMO, H., GOTO, A., SUGAMOTO, K. & YOSHIKAWA, H. 2009. Accuracy analysis of three-dimensional bone surface models of the forearm constructed from multidetector computed tomography data. *Int J Med Robot,* 5, 452-7.

OLLIVIER, M., PARRATTE, S., LE CORROLLER, T., REGGIORI, A., CHAMPSAUR, P. & ARGENSON, J. N. 2015. Anatomy of the proximal femur at the time of total hip arthroplasty is a matter of morphotype and etiology but not gender. *Surg Radiol Anat,* 37, 377-84.

PAHR, D. H. & ZYSSET, P. K. 2009. From high-resolution CT data to finite element models: development of an integrated modular framework. *Comput Methods Biomech Biomed Engin,* 12, 45-57.

PAN, Y.-Q., ZHENG, R., LIU, F.-B., JING, W., YONG, C., LIANG, X.-Y. & BING, W. 2014. The use of CT scan and stereo lithography apparatus technologies in a canine individualized rib prosthesis. *International Journal of Surgery,* 12, 71-75.

PATTON, M. S., DUTHIE, R. A. & SUTHERLAND, A. G. 2006. Proximal femoral geometry and hip fractures. *Acta orthopaedica belgica,* 72, 51.

PAUCHARD, Y., FITZE, T., BROWARNIK, D., ESKANDARI, A., PAUCHARD, I., ENNS-BRAY, W., PALSSON, H., SIGURDSSON, S., FERGUSON, S. J., HARRIS, T. B., GUDNASON, V. & HELGASON, B. 2016. Interactive graph-cut segmentation for fast creation of finite element models from clinical ct data for hip fracture prediction. *Comput Methods Biomech Biomed Engin,* 19, 1693-1703.

PAWASKAR, A. C., LEE, K. W., KIM, J. M., PARK, J. W., AMINATA, I. W., JUNG, H. J., CHUN, J. M. & JEON, I. H. 2012. Locking plate for proximal humeral fracture in the elderly population: serial change of neck shaft angle. *Clin Orthop Surg,* 4, 209-15.

PENG, L., BAI, J., ZENG, X. & ZHOU, Y. 2006. Comparison of isotropic and orthotropic material property assignments on femoral finite element models under two loading conditions. *Med Eng Phys,* 28, 227-33.

PINHEIRO, M. & ALVES, J. L. 2015. A New Level-Set-Based Protocol for Accurate Bone Segmentation From CT Imaging. *IEEE Access,* 3, 1894-1906.

PINSKY, H. M., DYDA, S., PINSKY, R. W., MISCH, K. A. & SARMENT, D. P. 2006. Accuracy of three-dimensional measurements using cone-beam CT. *Dentomaxillofac Radiol,* 35, 410-6.

References

RATHNAYAKA, K., MOMOT, K. I., NOSER, H., VOLP, A., SCHUETZ, M. A., SAHAMA, T. & SCHMUTZ, B. 2012. Quantification of the accuracy of MRI generated 3D models of long bones compared to CT generated 3D models. *Med Eng Phys,* 34**,** 357-63.

RAVICHANDRAN, D., MUTHUKUMARAVEL, N., JAIKUMAR, R., DAS, H. & RAJENDRAN, M. 2011. Proximal Femoral Geometry in Indians and its Clinical Applications. *Journal of Anatomical Society of India,* 60**,** 6-12.

RUBIN, P. J., LEYVRAZ, P. F., AUBANIAC, J. M., ARGENSON, J. N., ESTEVE, P. & DE ROGUIN, B. 1992. The morphology of the proximal femur. A three-dimensional radiographic analysis. *J Bone Joint Surg Br,* 74**,** 28-32.

SANTORE, R. F., TURGEON, T. R., PHILLIPS, W. F., 3RD & KANTOR, S. R. 2006. Pelvic and femoral osteotomy in the treatment of hip disease in the young adult. *Instr Course Lect,* 55**,** 131-44.

SARIALI, E., MOUTTET, A., PASQUIER, G., DURANTE, E. & CATONE, Y. 2009. Accuracy of reconstruction of the hip using computerised three-dimensional pre-operative planning and a cementless modular neck. *J Bone Joint Surg Br,* 91**,** 333-40.

SCHILEO, E., TADDEI, F., MALANDRINO, A., CRISTOFOLINI, L. & VICECONTI, M. 2007. Subject-specific finite element models can accurately predict strain levels in long bones. *J Biomech,* 40**,** 2982-9.

SCHINDELIN, J., ARGANDA-CARRERAS, I., FRISE, E., KAYNIG, V., LONGAIR, M., PIETZSCH, T., PREIBISCH, S., RUEDEN, C., SAALFELD, S., SCHMID, B., TINEVEZ, J.-Y., WHITE, D. J., HARTENSTEIN, V., ELICEIRI, K., TOMANCAK, P. & CARDONA, A. 2012. Fiji: an open-source platform for biological-image analysis. *Nature Methods,* 9**,** 676.

SCHNURR, C., NESSLER, J., MEYER, C., SCHILD, H. H., KOEBKE, J. & KONIG, D. P. 2009. Is a valgus position of the femoral component in hip resurfacing protective against spontaneous fracture of the femoral neck?: a biomechanical study. *J Bone Joint Surg Br,* 91**,** 545-51.

SCHUMANN, S., TANNAST, M., NOLTE, L.-P. & ZHENG, G. 2010. Validation of statistical shape model based reconstruction of the proximal femur—A morphology study. *Medical Engineering & Physics,* 32**,** 638-644.

SHU, D.-L., LIU, X.-Z., GUO, B., RAN, W., LIAO, X. & ZHANG, Y.-Y. 2014. Accuracy of using computer-aided rapid prototyping templates for mandible reconstruction with an iliac crest graft. *World journal of surgical oncology,* 12**,** 190-190.

SOODMAND, E., KLUESS, D., VARADY, P. A., CICHON, R., SCHWARZE, M., GEHWEILER, D., NIEMEYER, F., PAHR, D. & WOICZINSKI, M. 2018. Interlaboratory comparison of femur surface reconstruction from CT data compared to reference optical 3D scan. *Biomed Eng Online,* 17**,** 29.

SOODMAND, E., NATSAKIS, T., JONKERS, I. & VANDER SLOTEN, J. Intra-articular Pressure Based Stress Analysis of the Distal Tibia Following Insertion of a Total Ankle Replacement. Computer Methods in Biomechanics and Biomedical Engineering, Date: 2015/09/01-2015/09/05, Location: Montreal, Canada, 2015. Taylor & Francis.

SRIMATHI, T., MUTHUKUMAR, T., ANANDARANI, V., UMAPATHY, S. & RAMESHKUMAR, S. 2012. A study on femoral neck anteversion and its clinical correlation. *J Clin Diagn Res,* 6**,** 155-158.

TAYLOR, M. & PRENDERGAST, P. J. 2015. Four decades of finite element analysis of orthopaedic devices: Where are we now and what are the opportunities? *Journal of Biomechanics,* 48**,** 767-778.

THEVENOT, J., KOIVUMAKI, J., KUHN, V., ECKSTEIN, F. & JAMSA, T. 2014. A novel methodology for generating 3D finite element models of the hip from 2D radiographs. *J Biomech,* 47**,** 438-44.

TONNIS, D. & HEINECKE, A. 1999. Acetabular and femoral anteversion: relationship with osteoarthritis of the hip. *J Bone Joint Surg Am,* 81**,** 1747-70.

TRABELSI, N., YOSIBASH, Z., WUTTE, C., AUGAT, P. & EBERLE, S. 2011. Patient-specific finite element analysis of the human femur--a double-blinded biomechanical validation. *J Biomech,* 44**,** 1666-72.

TREECE, G. M., PRAGER, R. W. & GEE, A. H. 1999. Regularised marching tetrahedra: improved iso-surface extraction. *Computers & Graphics,* 23**,** 583-598.

VÄÄNÄNEN, S. P., ISAKSSON, H., JULKUNEN, P., SIROLA, J., KRÖGER, H. & JURVELIN, J. S. 2011. Assessment of the 3-D shape and mechanics of the proximal femur using a shape template and a bone mineral density image. *Biomechanics and Modeling in Mechanobiology,* 10**,** 529-538.

VAN DEN BROECK, J., VEREECKE, E., WIRIX-SPEETJENS, R. & VANDER SLOTEN, J. 2014. Segmentation accuracy of long bones. *Med Eng Phys,* 36**,** 949-53.

VERIM, Ö., TAŞGETIREN, S., ER, M. S., TIMUR, M. & YURAN, A. F. 2013. Anatomical comparison and evaluation of human proximal femurs modeling via different devices and FEM analysis. *The International Journal of Medical Robotics and Computer Assisted Surgery,* 9**,** e19-e24.

VO, A., BEAULE, P. E., SAMPAIO, M. L., ROTARU, C. & RAKHRA, K. S. 2015. The femoral head-neck contour varies as a function of physeal development. *Bone Joint Res,* 4**,** 17-22.

WAANDERS, D., JANSSEN, D., MANN, K. A. & VERDONSCHOT, N. 2011. Morphology based cohesive zone modeling of the cement–bone interface from postmortem retrievals. *Journal of the Mechanical Behavior of Biomedical Materials,* 4**,** 1492-1503.

WANG, J., YE, M., LIU, Z. & WANG, C. 2009. Precision of cortical bone reconstruction based on 3D CT scans. *Comput Med Imaging Graph,* 33**,** 235-41.

WANG, L. I., GREENSPAN, M. & ELLIS, R. 2006. Validation of bone segmentation and improved 3-D registration using contour coherency in CT data. *IEEE Trans Med Imaging,* 25**,** 324-34.

WEINANS, H., HUISKES, R. & GROOTENBOER, H. J. 1994. Effects of fit and bonding characteristics of femoral stems on adaptive bone remodeling. *J Biomech Eng,* 116**,** 393-400.

WHITE, D., CHELULE, K. L. & SEEDHOM, B. B. 2008. Accuracy of MRI vs CT imaging with particular reference to patient specific templates for total knee replacement surgery. *Int J Med Robot,* 4**,** 224-31.

WILLMOTT, C. J., ACKLESON, S. G., DAVIS, R. E., FEDDEMA, J. J., KLINK, K. M., LEGATES, D. R., O'DONNELL, J. & ROWE, C. M. 1985. Statistics for the evaluation and comparison of models. *Journal of Geophysical Research: Oceans,* 90**,** 8995-9005.

WOOLF, A. D. & PFLEGER, B. 2003. Burden of major musculoskeletal conditions. *Bull World Health Organ,* 81**,** 646-56.

YOO, M. C., CHO, Y. J., CHUN, Y. S. & RHYU, K. H. 2011. Impingement between the acetabular cup and the femoral neck after hip resurfacing arthroplasty. *J Bone Joint Surg Am,* 93 Suppl 2**,** 99-106.

ZHENG, G., HOMMEL, H., AKCOLTEKIN, A., THELEN, B., STIFTER, J. & PEERSMAN, G. 2018. A novel technology for 3D knee prosthesis planning and treatment evaluation using 2D X-ray radiographs: a clinical evaluation. *Int J Comput Assist Radiol Surg,* 13**,** 1151-1158.

ZYSSET, P., PAHR, D., ENGELKE, K., GENANT, H. K., MCCLUNG, M. R., KENDLER, D. L., RECKNOR, C., KINZL, M., SCHWIEDRZIK, J., MUSEYKO, O., WANG, A. & LIBANATI, C. 2015. Comparison of proximal femur and vertebral body strength improvements in the FREEDOM trial using an alternative finite element methodology. *Bone,* 81**,** 122-130.

10 Summary of Original Papers for the Cumulative Dissertation

The following original papers were used for this cumulative dissertation:

10.1 Study 1

Surgically Relevant Morphological Parameters of Proximal Human Femur: A Statistical Analysis Based on 3D Reconstruction of CT Data

Ehsan Soodmand, MSc[1], Guoyan Zheng, PhD[2], Wolfram Steens, MD[1], Rainer Bader, MD, PhD[1], Lutz Nolte, PhD[2], Daniel Kluess, PhD[1]

[1]Department of Orthopaedics, University Medicine of Rostock, Rostock, Germany and [2]Institute for Surgical Technology and Biomechanics, University of Bern, Bern, Switzerland.

Summary

Objectives: Recently, more accurate description of the femoral geometry has become of interest to engineers and orthopaedic surgeons. However, an appropriate database is lacking. Therefore, the aim of this study is to present morphological parameters and their correlations, which are relevant for medical issues such as impingement after total hip replacement, as well as for implant design and the aetiology of hip fractures.

Methods: We investigated 12 well-known morphological parameters of the femur in 169 healthy human subjects through evaluation of 3D-reconstructed CT scans. Pearson's coefficients of correlations were calculated using a statis- tical t-test method for each pair of parameters.

Results: The mean, maximum, minimum, median, and standard deviation values are reported for all parameters. Histograms showing the distribution of each morphological parameter are also presented. It is shown that absolute and horizontal offsets, total femur length, and NCVD parameters are normally distributed, but NCDF and NCDS are not. Furthermore, an inter-correlation matrix was reported to reveal statistical correlations between these parameters. The strongest positive correlation existed between absolute offset (OSA) and horizontal offset (OSH), while the least positive correlation was found between NCDF and total femur length (TFL), and also between NCDS and NCDF. Anteversion angle (ATA) and OSA showed the least negative correlation. However, the strongest negative correlation was found between neck-shaft angle (NSA) and greater trochanter height (GTH), as well as between OSA and NCVD.

Conclusions: Comprehending patients' native bone morphology, including the variations and correlations, is essential for orthopaedic surgeons to undertake preoperative planning and surgery as well as to appropriately design medical devices. Thus, more population-based detailed databases are necessary. We investigated an extensive set of proximal femoral morphology parameters using a statistically standardized method to expand the existing knowledge. The results of our study can be used for diverse medical and biomechanical purposes.

Key words: Femur morphology; Hip joint; Impingement; Morphological study; Proximal femur

10.2 Study 2

Interlaboratory comparison of femur surface reconstruction from CT data compared to reference optical 3D scan

Ehsan Soodmand[1]*, Daniel Kluess[1], Patrick A. Varady[2], Robert Cichon[3], Michael Schwarze[4], Dominic Gehweiler[5], Frank Niemeyer[6], Dieter Pahr[7], and Matthias Woiczinski[8]

[1]Biomechanics and Implant Technology Research Laboratory, Department of Orthopaedics, University Medicine Rostock, Doberaner Strasse 142, 18057 Rostock, Germany.

[2]Trauma Center Murnau Institute of Biomechanics, Professor-Küntscher-Str. 882418, Murnau am Stafelsee, Germany.

[3]Chair of Mechanics and Robotics, University DuisburgEssen, Lotharstrasse 1, 47057 Duisburg, Germany.

[4]Laboratory for Biomechanics and Biomaterials of the Orthopaedic Clinic, Hannover Medical School, Anna-von-Borries-Strasse 1-7, 30625 Hannover, Germany. [5]Department of Trauma, Hand and Reconstructive Surgery, University Hospital Münster, Albert-Schweitzer-Campus 1, 48149 Münster, Germany.

[6] Fraunhofer Research Institution for Large Structures in Production Engineering (IGP), Albert-Einstein-Str. 30, 18059 Rostock, Germany.

[7]Institute of Lightweight Design and Structural Biomechanics, TU Vienna, Getreidemarkt 9, 1060 Vienna, Austria.

[8]Department of Orthopedic Surgery, Physical Medicine and Rehabilitation, University Hospital of Munich (LMU), Marchioninistr. 15, 81377 Munich, Germany.

Summary

Background: The present study contrasts the accuracy of different reconstructed models with distinctive segmentation methods performed by various experts. Seven research groups reconstructed nine 3D models of one human femur based on an acquired CT image using their own computational methods. As a reference model for accuracy assessment, a 3D surface scan of the human femur was created using an optical measuring system. Prior to comparison, the femur was divided into four areas; "neck and greater trochanter", "proximal metaphysis", "diaphysis", and "distal metaphysis". The deviation analysis was carried out in GEOMAGIC studio v.2013 software.

Results: The results revealed that the highest deviation errors occurred in "neck and greater trochanter" area and "proximal metaphysis" area with RMSE of 0.84 and 0.83 mm respectively.

Conclusion: In conclusion, this study shows that the average deviation of reconstructed models prepared by experts with various methods, skills and software from the surface 3D scan is lower than 0.79 mm, which is not a significant discrepancy.

Keywords: Accuracy assessment, Deviation analysis, Image-based model, Bone segmentation, Shape reconstruction, Medical imaging, Round robin test

10.3 Study 3

A round-robin finite element analysis of human femur mechanics between seven participating laboratories with experimental validation

Daniel Kluess[a], Ehsan Soodmand[a], Andrea Lorenz[b], Dieter Pahr[b], Michael Schwarze[c], Robert Cichon[d], Patrick A. Varady[e], Sven Herrmann[e], Bernhard Buchmeier[f], Christian Schröder[g], Stefan Lehner[h] & Maeruan Kebbach[a]

[a]Department of Orthopaedics, Rostock University Medical Center, Rostock, Germany.

[b]TU Wien Institute of Lightweight Design and Structural Biomechanics, Vienna, Austria.

[c]Department of Orthopaedic Surgery, Hannover Medical School, Hannover, Germany.

[d]Chair of Mechanics and Robotics, University of Duisburg-Essen, Duisburg, Germany.

[e]BG Unfallklinik Murnau Institute for Biomechanics, Murnau am Staffelsee, Germany.

[f]TÜV SÜD Industrie Service GmbH, Müunchen/Munich, Germany.

[g]Orthop€adie & Traumatologie/ Orthopedics & Traumatology, TÜV SÜD Product Service GmbH, Müunchen/Munich, Germany.

[h]Faculty Mechanical Engineering and Mechatronics, Deggendorf Institute of Technology, Deggendorf, Germany.

Summary

Finite element analysis is a common tool that has been used for the past few decades to predict the mechanical behaviour of bone. However, to our knowledge, there are no round-robin finite element analyses of long human bones with more than two participating biomechanics laboratories published yet, where the results of the experimental tests were not known in advance. We prepared a fresh-frozen human femur for a compression test in a universal testing machine measuring the strains at 10 bone locations as well as the deformation of the bone in terms of the displacement of the loading point at a load of 2 kN. The computed tomography data of the bone with a calibration phantom as well as the orientation of the bone in the testing machine with the according boundary conditions were delivered to seven participating laboratories. These were asked to perform a finite element analysis simulating the experimental setup and deliver their results to the coordinator without knowing the experimental results. Resultantly, four laboratories had deviations from the experimentally measured strains of less than 40%, and three laboratories had deviations of their numerically determined values compared to the experimental data of more than 120%. These deviations are thought to be based on different material laws and material data, as well as different material mapping methods. Investigations will be conducted to clarify and assess the reasons for the large deviations in the numerical data. It was shown that the precision of finite element models of the human femur is not yet as developed as desired by the biomechanics community.

Keywords: Round robin, finite element analysis, femur, compression test, musculoskeletal

11 Acknowledgment

Throughout the writing of this dissertation I have received a great deal of support and assistance. I would first like to express my deepest appreciation to my supervisors, Prof. Dr. med. habil. Dipl.-Ing. Rainer Bader, and PD Dr.-Ing. habil. Daniel Klüß for their support. Working with Rainer was a real pleasure as I learned a lot from him. Despite his busy agenda, he was there for me whenever I needed his advice on both research and personal matters. Daniel's supervision was very invaluable to me, and without his guidance and persistent help, this dissertation would not have been possible.

I would like to extend my acknowledgements to my dear colleagues, Mr. Märuan Kebbach, Mr. Andreas Geier, and Ms. Anne-Marie Neumann for their support over these years.

I would also like to thank all of my research partners, who contributed in writing the articles and provided me with worthy feedback and suggestions to improve the quality of the manuscripts such as Univ.-Prof. DI Dr. Dieter Pahr, Prof. Dr. Guoyan Zheng, and Dr. Wolfram Steens.

I would like to thank the institutes contributed in our Round robin and benchmark studies; TU Wien Institute of Lightweight Design and Structural Biomechanics, Vienna, Austria, Department of Orthopaedic Surgery, Hannover Medical School, Hannover, Germany, Chair of Mechanics and Robotics, University of Duisburg-Essen, Duisburg, Germany, BG Unfallklinik Murnau Institute for Biomechanics, Murnau am Staffelsee, Germany, Faculty Mechanical Engineering and Mechatronics, Deggendorf Institute of Technology, Deggendorf, Germany, Department of Trauma, Hand and Reconstructive Surgery, University Hospital Münster, Germany, and Fraunhofer Research Institution for Large Structures in Production Engineering (IGP), Rostock, Germany.

A very special gratitude goes out to some amazing people without whom I would not be able to complete this work:

My wife, Melika, for her patience and emotional support in my life, and putting up with me being busy and not available most of the time due to the workload for such a long time. In addition, she always supported me with proof reading of my dissertation, and in deliberating over my problems and findings, as well as providing happy distraction to rest my mind outside of my research.

My brother for being spiritually by my side and giving me suggestions with his distinctive calm attitude dealing with critical situations.

My parents for believing in me and for their unconditional support and sympathetic ear. They have always been proud of me for my academic achievement and I am now indescribably delighted to make them feel this way again by accomplishing my doctorate degree.

And finally, last but by no means least, my grandparents who love me unconditionally. I could not have finished any of this without you. Thanks for all your encouragement!

12 Curriculum Vitae

Ehsan Soodmand

University Education

04/2016 – 07/2020 — **PhD** – **Biomedical Engineering,** Biomechanics and Implant Technology Research Laboratory Universitätsmedizin Rostock, Rostock, Germany.

- Project: Biomechanical importance of proximal human femur morphology and mechanics in orthopedic purposes.

04/2010 – 07/2012 — **Master** – **Biomedical Engineering,** University of Malaya, Kuala Lumpur, Malaysia.

- Project: The controlling of dynamic parameters of knee joint in transfemoral amputee gait.

09/2004 – 09/2008 — **Bachelor** – **Mechanical Engineering,** IA University of Ahvaz, Ahvaz, Iran.

- Project: Analyzing and designing of a packing machine for powder products.

Professional Background (Underlined texts are hyperlinked)

Since 01/2017 — **Research associate, Charité - Universitätsmedizin Berlin**, Julius Wolff Institute for Biomechanics and Musculoskeletal Regeneration, Berlin, Germany.

- Project: Mechanically driven cellular self-organization and soft tissue patterning in bone healing.

Since 09/2018 (Part Time) — **Employee for technology, service and administration, Humboldt Universität zu Berlin**, Humboldt Graduate School, Key Competencies and Mentoring.

09/2015 – 12/2016 — **Research associate, Universitätsmedizin Rostock**, Biomechanics and Implant Technology Research Laboratory (FORBIOMIT), Department of Orthopedics, Rostock, Germany.

- Project: Numerical analysis of lower limb joints and tissues in orthopedics biomechanics.
- (Co-developer of a successful DFG grant (Project Number: 385973984)).

07/2013 – 08/2015 — **Teaching assistant and research associate, Technical University of Chemnitz**, Institute of Human Movement Science, Chemnitz, Germany.

- Teaching: Basic Biomechanics.
- Project: Finite element analysis of human foot and ankle joint.

06/2012 – 04/2013 — **Research associate, University of Malaya**, Faculty of Dentistry, Kuala Lumpur, Malaysia.

- Project: Finite element analysis of maxillary expander.

04/2011 – 08/2011 — **Asset Integrity Engineer, Germanischer Lioyd Noble Denton**, Kuala Lumpur, Malaysia.

- Scheduling a preventive maintenance for the equipment according to failure mode effect analysis (FMEA) standard using risk-based inspection software.

06/2008 – 04/2010 — **Project Engineer**, Tasha Manufacturing Company, Ahvaz, Iran.

- Managing engineering and fabrication aspects of fixed equipment for oil and petrochemical industries according to American Petroleum Institute (API) standards.

09/2007 – 05/2010	**Project manager**, [Elm O Sanat E Aria](#) **Educational Institute**, Ahvaz, Iran.

- Leading a group of three employees to mechanize the administration system.

Mobility Projects

Since 02/2020	**Eindhoven University of Technical**, [Soft Tissue Engineering and Mechanobiology Institute](#), Eindhoven, Netherlands.

- Project: Mechanically driven and cell mediated collagen fiber deposition, reorientation in bone defect healing.

02/2015 – 04/2015	**Katholieke Universiteit Leuven**, [Division of Biomechanics, Leuven](#), Belgium.

- Project: Finite element stress analysis of maximum pressure of ankle joint during walking using Hintegra total ankle replacement.

Achievement and Awards

07/2020	**Best Student Award** – Runnerup - European Society of Biomechanics (ESB).
07/2019	**Mobility Award** – Research collaboration with Eindhoven University of Technical European Society of Biomechanics.
04/2019	**Travel Award** – Deutsche Gesellschaft für Biomechanik (DGfB).
12/2018 & 12/2017	**Best Poster Presentation Award** – BSRT (Charité) symposium 2018 and 2017.
07/2017	**Travel Award** – European Molecular Biology Organization (excellence in the life sciences).
2017 – 2018	**Friede Springer Stiftung** – Two-years funding for a research project at Charité Universitaetsmedizin Berlin in the field of regenerative therapies (Bone Healing).
09/2015	**Travel Award** – CMBBE2015, Montreal, Canada – InPro TUC.
2014 – 2015	**DAAD (Matching Fund)** – Two years Stipend for Research in field of Biomechanics.

Technical Skills

Management Tools	Microsoft Project, SAP, Trello, Endnote, Mind Mapping tools.
Remote Tools	Microsoft Desktop Remote, AnyDesk, Team Viewer, Microsoft Team, GoToMeeting, Zoom, Skype, Cloud System (Dropbox, Google Drive, etc.).
Programming Skills	C++, Matlab, R.
Technical Analysis & Modelling Software	Abaqus, FEBio, Solidworks, ImageJ, AnyBody Modeling, Vicon MX, Geomagic Studio, Seg3D, Mimics Innovation Suite, Amira, OsiriX Lite, Origin Pro.
Cell Culture and Biomechanical skills	3D cell culture, Immunohistochemistry, histology, confocal microscopy, SEM Imaging, cryostat sectioning, mechanical tests using Bose, Instron, and Zwick/Roell machines.
General PC Skills	Microsoft Office, Google tools, Windows, Mac iOS, Gimp, Photoshop, Prezi, OBS, Camtasia.

Peer-reviewed Publications and International Conferences

Publications	Author and Coauthor in 8 peer-reviewed publications, 84 citations, H-index 5

- Please visit my Google Scholar profile **([Google Scholar Profile](#))**.

Presentations	9 podium and 5 poster presentations in 9 different countries

- Fields: Orthopeadic Biomechanics and/or Mechanical engineering.

Leadership Activities and Social Management

01/2019 – 12/2019	**Co-organizer** – [BSRT regenerative medicine symposium](#) 2019.
Since 2018	**Webinar Organizer and Student Representative**, European Society of Biomechanics.
07/2017 & 07/2019	**Co-chair** of "Computational Biomechanics" and "Hard Tissue Biomechanics "sessions at 25th ESB congress, Vienna, Austria and 23rd congress of ESB, Seville, Spain.
Since 2004	**Futsal Player** – Former Captain at University Team and currently semi-professional player in Berlin Landesliga (ASV Berlin).
2011 – 2013	**Elected President** – University of Malaya International Student Association.
2010 – 2012	**Student Representative** – Biomedical Eng. Students at University of Malaya.

Selected Advanced Career Development and Trainings

02/2020	Results-based project management: monitoring and evaluation. Online course at edX.org.
01/2020	Managing Projects with Microsoft Project, Online course at edX.org.
11/2019	Speaking with confidence and impact, Humboldt Graduate School, Berlin, Germany.
02/2019	Clinical rotation at Center for Musculoskeletal Surgery, Charité - Universitätsmedizin, Berlin, Germany (4 weeks).
09/2018	From Protein to Tissue to Organ: Modelling and Computation, TU Graz, Austria.
11/2017	Histology of bone regeneration, Charité - Universitätsmedizin Berlin.
07/2017	Multilevel modelling of morphogenesis, European Molecular Biology Organization, John Innes Centre, Norwich Research Park, UK.
07/2017	Bone cell and tissue mechanics, International Centre for Mechanical Sciences (CISM), Udine, Italy.
09/2015	Statistical analysis with R, online course at edX.org.
07/2014	Medical 3D Modeling for finite element analysis, Mimics innovation course, Galerie de Paléontologie et d'Anatomie comparée, Paris, France.

Language Skills

English	Fluent (IETLS Academic 6.5).
German	Full professional proficiency (C1).
Persian	Native speaker.
Arabic	Basic (A2 Level).

Personal Skills

Soft skills	Highly Tech Savvy, Extroverted and communicative, Excellent presentation skills, Persuasive speaker, Team player.
Driving license	B, full clean driving license.
Hobbies	Traveling, playing football, dining out, listening to podcasts, reading books.

12.1 List of Publications

- Kluess, D., **Soodmand, E.,** Lorenz, A., Pahr, D., Schwarze, M., Cichon, R., Varady, P., Herrmann, S., Buchmeier, B., Lehner, S., Kebbach, M. A round-robin finite element analysis of human femur mechanics between seven participating laboratories with experimental validation. Comput Methods Biomech Biomed Engin 2019 22(12): 1020-1031. doi:10.1080/10255842.2019.1615481.

- Geier, A., Kebbach, M., **Soodmand, E.**, Woernle, C., Kluess, D., & Bader, R. (2019). Neuro-musculoskeletal flexible multibody simulation yields a framework for efficient bone failure risk assessment. Sci Rep, 9(1), 6928. doi:10.1038/s41598-019-43028-6

- **Soodmand, E.,** Zheng, G., Steens, W., Bader, R., Nolte, L., & Kluess, D. (2019). Surgically Relevant Morphological Parameters of Proximal Human Femur: A Statistical Analysis Based on 3D Reconstruction of CT Data. Orthop Surg. doi:10.1111/os.12416

- **Soodmand, E.,** D. Kluess, P. A. Varady, R. Cichon, M. Schwarze, D. Gehweiler, F. Niemeyer, D. Pahr and M. Woiczinski (2018). "Interlaboratory comparison of femur surface reconstruction from CT data compared to reference optical 3D scan." BioMedical Engineering OnLine 17(1): 29.

- Ahmady, A., **Soodmand, E.*,** Soodmand, I., Milani, TL. The effect of various heights of high-heeled shoes on foot arch deformation: Finite element analysis. Journal of Foot and Ankle Research, 2014. 7(Suppl 1): p. A78

- Eshraghi, A., Abu Osman, N. A., Karimi, M., Gholizadeh, H., **Soodmand, E.,** & Wan Abas, W. A. (2014). Gait biomechanics of individuals with transtibial amputation: effect of suspension system. PLoS One, 9(5), e96988. doi:10.1371/journal.pone.0096988.

- Moradi, A., Nafchi, A. M., Ghanbarzadeh, A., & **Soodmand, E.** (2011, 5-6 Dec. 2011). Optimization of linear and nonlinear full vehicle model for improving ride comfort vs. road holding with the Bees Algorithm. Paper presented at the 2011 IEEE Colloquium on Humanities, Science and Engineering.

- Nafchi, A. M., Moradi, A., Ghanbarzadeh, A., Rezazadeh, A., & **Soodmand, E.** (2011, 5-6 Dec. 2011). Solving engineering optimization problems using the Bees Algorithm. Paper presented at the 2011 IEEE Colloquium on Humanities, Science and Engineering.

12.2 Conference Proceedings

- **Soodmand E.,** Duda G.N., Petersen A., Checa S., Mechanically driven cellular self-organization as a mechanism driving large bone defect healing. European Society of Biomechanics Congress, **ESB2020**.

- **Soodmand E.,** Duda G.N., Petersen A., Checa S., The influence of geometrical constraints on cellular self-organization during the early stages of bone healing. European Society of Biomechanics Congress, **ESB2019**, Vienna, Austria

- **Soodmand E.,** Duda G.N., Petersen A., Checa S., The influence of mechanical stimuli on cellular self-organization during the early stages of bone healing. German Society of Biomechanics Conference, **DGfB2019**, Berlin, Germany.

- **Soodmand E.**, Duda G.N., Petersen A., Checa S., Mechanical interactions between cells and extracellular matrix during early stage of bone healing. **BSRT PhD Symposium 2018**, Berlin, Germany

- **Soodmand E.,** Duda G.N., Petersen A., Checa S., Mechanical interactions between cells and extracellular matrix during early stages of bone healing. World congress of Biomechanics 2018 **(WCB2018)**, Dublin, Ireland.

- **Soodmand E.**, Duda G.N., Petersen A., Checa S., Mechanically Driven Cellular Self-Organization and Soft Tissue Patterning in Bone Defect Healing, **BSRT PhD Symposium 2017,** Berlin, Germany.

- **Soodmand E**., Kluess, D., Varady P., Cichon, R., Schwarze M., Gehweiler, D., Pahr, D., Woiczinski, M., Benchmark Accuracy Assessment of CT Image-Based Reconstructed Human Femur Using 3D Optical Scan. 23rd Congress of the European Society of Biomechanics, July 2-5, 2017 **(ESB2017)**, Seville, Spain.
- **Soodmand, E.,** Kebbach, M., Geier, A., Bader, R., Kluess, D. A two-way FEA validation of the human femur by optical scan data and strain measurement. Orthopaedic Research Society 2017 **(ORS2017)** Annual Meeting, San Diego, California, USA.
- Geier, A., Kebbach, M., **Soodmand, E.,** Kluess, D., Bader, R. Computational Modeling of a Proximal Femur: A Benchmark Test between Finite-Element Analysis and Flexible Multibody Simulation. European Congress on Computational Methods in Applied Sciences and Engineering **(ECCOMAS2016),** Crete Island, Greece.
- **Soodmand, E.,** Natsakis, T., Jonkers, I., Vander Sloten, J. Stress analysis of maximum pressure of ankle joint during walking using Hintegra total ankle replacement using finite element modeling. 13th International Symposium on Computer Methods in Biomechanics and Biomedical Engineering **(CMBBE 2015),** Montreal, Canada.